



**The Abdus Salam  
International Centre for Theoretical Physics**



**1936-50**

**Advanced School on Synchrotron and Free Electron Laser Sources  
and their Multidisciplinary Applications**

*7 - 25 April 2008*

**Application of x-ray imaging in Medicine**

Giuliana Tromba  
*Sincrotrone  
Trieste*

---

# Application of x-ray imaging in medicine

*Giuliana Tromba*

*Sincrotrone Trieste*

*SYRMEP Collaboration*

# Some applications at SYRMEP

<b>Technique</b>	<b>Applications</b>
Absorption	<b>Bones</b> , teeth studies
Contrast agent-based imaging (tracking studies using heavy elements, K or L edge imaging)	Angiography, bronchography, <b>brain studies(^)</b>
Phase Contrast imaging (PHC)	<b>Mammography, lungs</b>
Diffraction Enhanced Imaging (DEI)	<b>Cartilages, joints</b> , lungs, etc

(^) in combination with PHC imaging

## I

# Cell tracking studies for imaging of brain tumors in rats

Technique: Contrast agent (Gd) + PHC

Image modality: micro-CT

# Imaging of Brain Tumors

Glioblastoma multiforme (GBM) is the most common and most aggressive primary brain tumor in humans.

One reason for the high rate of recurrence is the invasive nature of the tumor into the surrounding normal brain tissue and its multifocal occurrence at sites remote from that of the primary tumor.

Animal model based on Wistar rats have been developed to study the behavior of the tumor and to monitor the effects of therapies.

Requirements for the cell tracking technique:

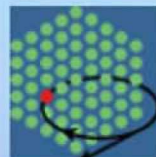
- to monitor the dynamic of tumour growth
- to follow the migration of tumour cells
- to understand the dynamic of metastasis spread



Section of healthy rat brain



Section of rat brain with C6 glioma 2 weeks after implantation



Sir Charles Gairdner Hospital



MONASH University

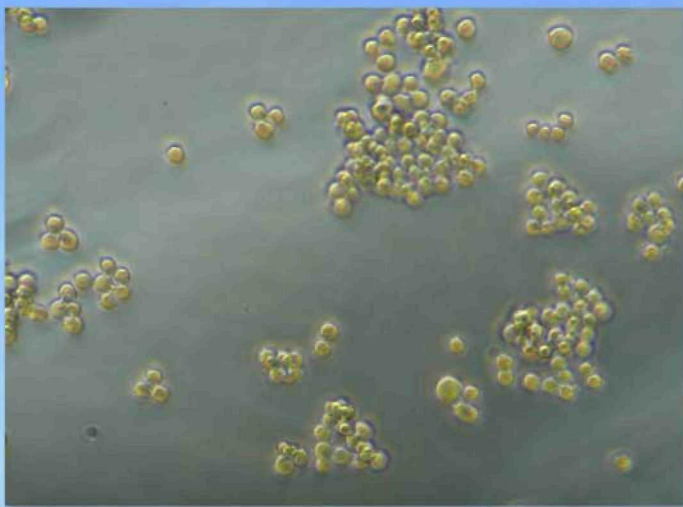


## Imaging of Brain Tumor

C6 glioma cells were cultured and some of the cultures were exposed to colloidal Gold Nano Particles (GNP) for 22 hrs before harvest.

C6 glioma cells were implanted into the brain of adult male Wistar rats. The implantation was performed with the animals under general anesthesia. The animals were allowed to recover after the end of the implantation and were sacrificed two weeks later.

We then employed SR CT technique to image the tumor. The detection of labeled cells is enhanced by the higher absorption of gold with respect to tissue and by PHC effects.



Gold Nano particles (GNP)

Our biological approach: Label cells with sufficient Au nano particles (  $\text{\O} \sim 50 \text{ nm}$  )

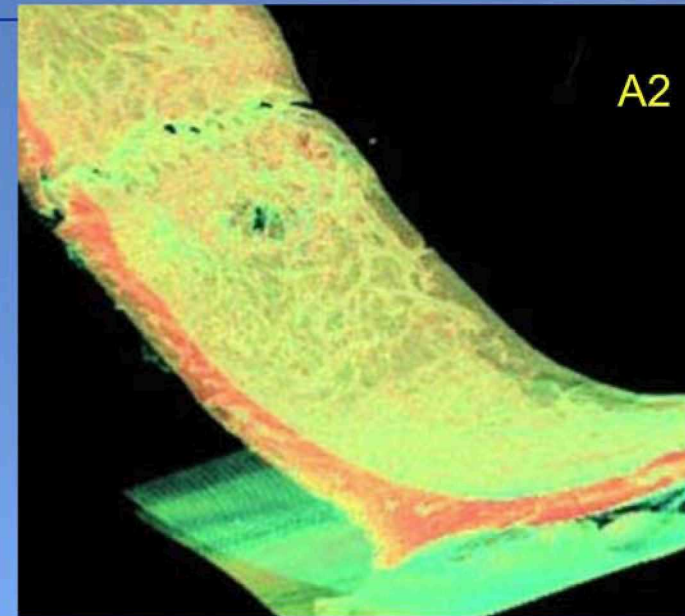
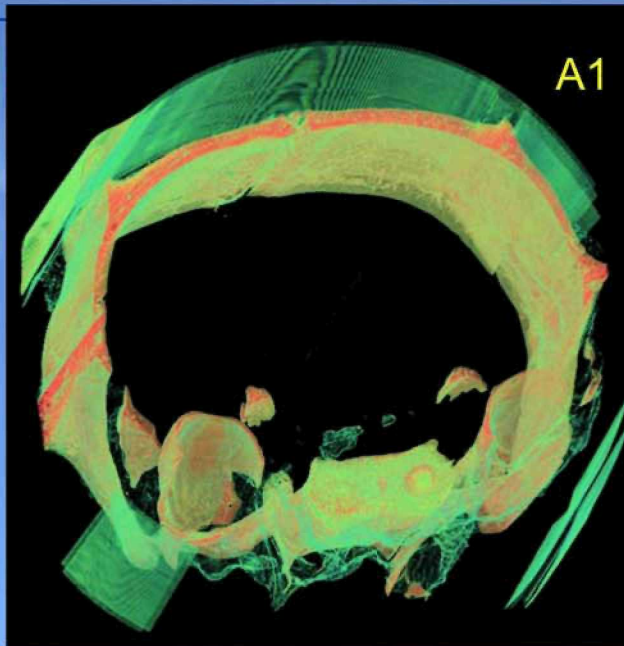
Inert GNP bond to serum proteins

GNP are taken up by phagocytosis stored in lysosomes and are not released by exocytosis

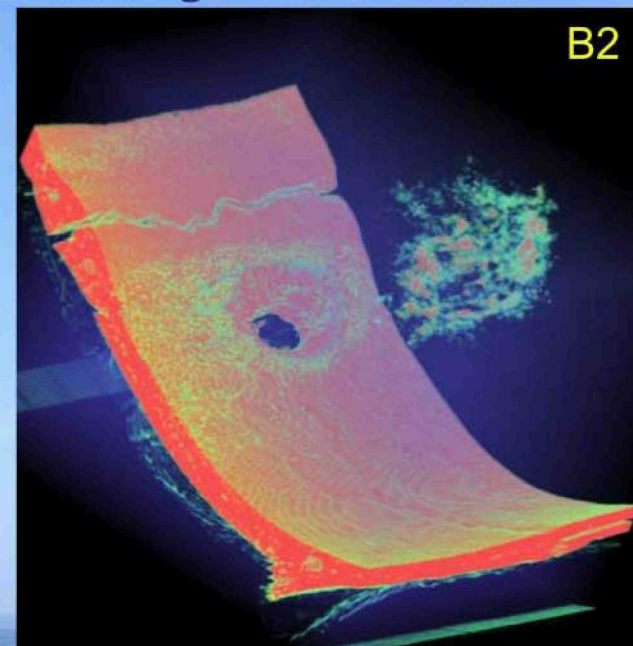
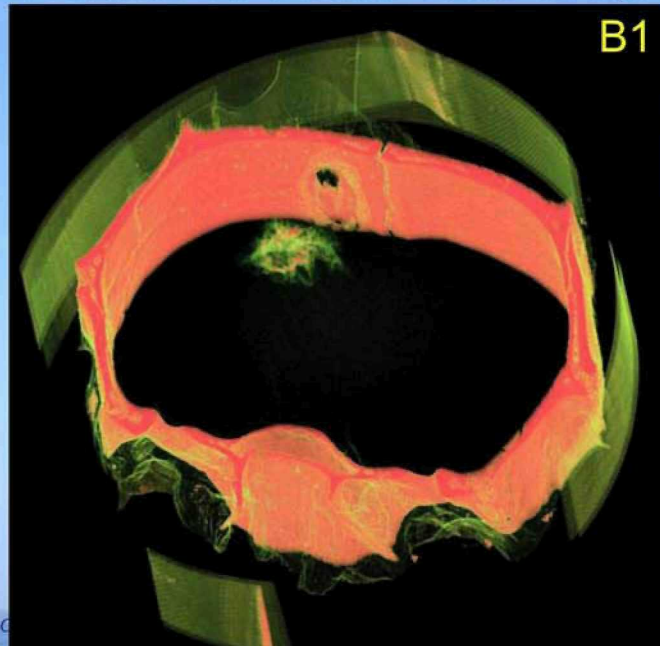
### A 1 and A 2: Tumor without colloidal gold

3D rendering of a  
4 mm thick  
volume

E = 24 keV  
Num. proj. = 720  
Pixel size = 14 $\mu$ m



### B 1 and B 2: Tumor with 300,000 colloidal gold-loaded cells



## II

# Mammography: in vivo trial with patients

Technique: PHC

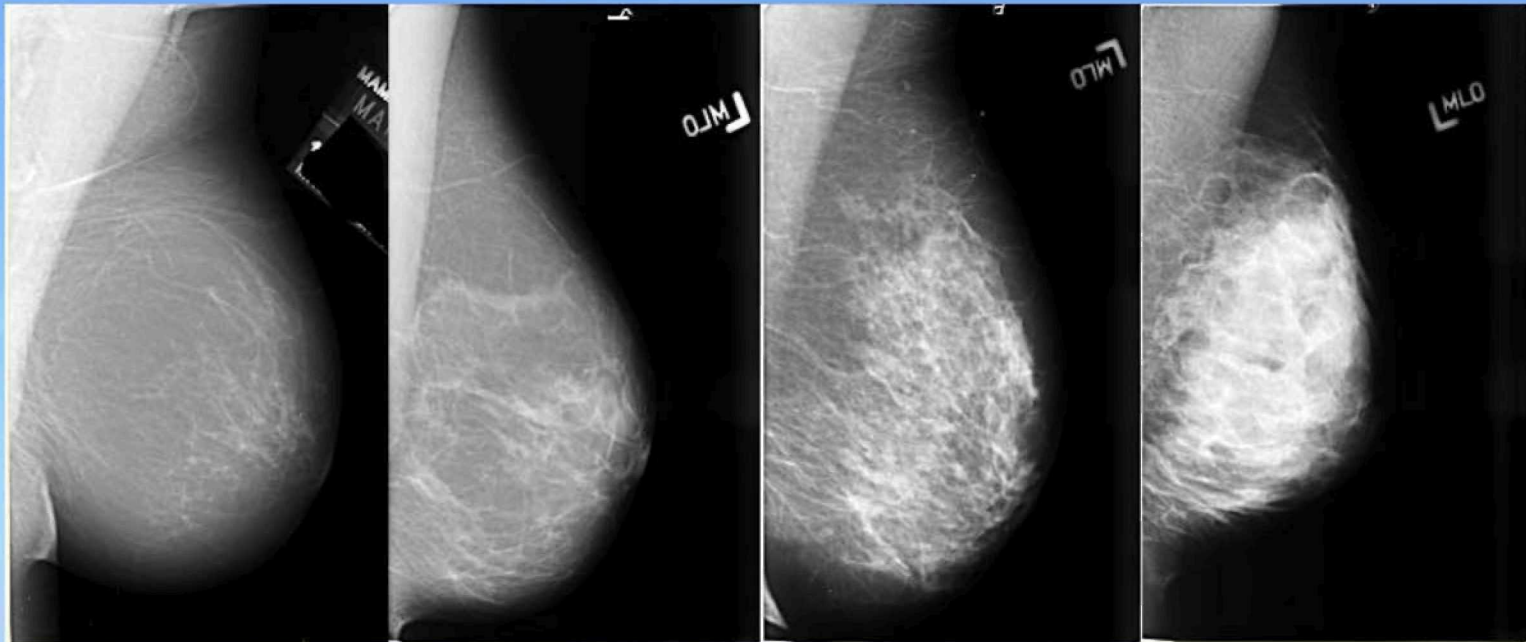
Image modality: planar



# Breast imaging

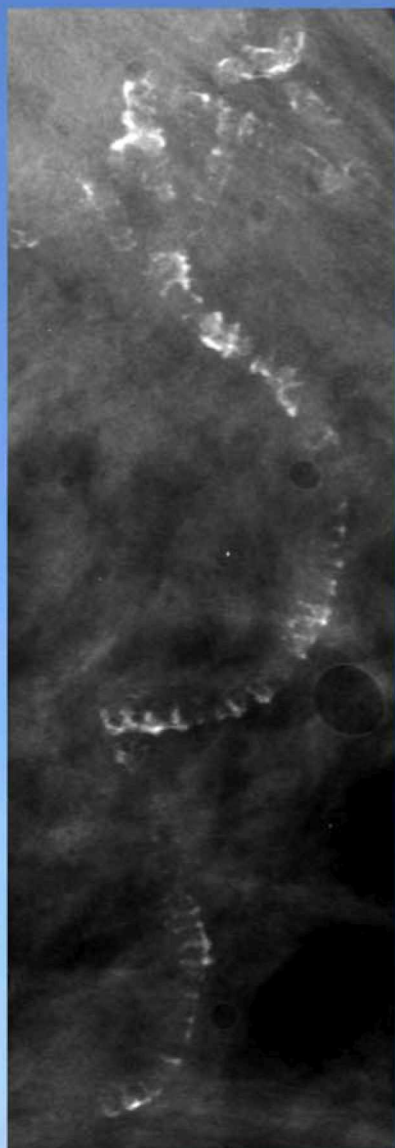
- Breast cancer is the most common cancer amongst women (incidence: 8%)
- The success of treatment depends on early detection (asymptomatic women)
- Main method for detecting early breast -> **X-ray mammography**
- Screening programs for large population area above 50 years old
- Sensitivity of conventional mammography: 85-90%, Specificity: 90%
- False positive/true positive  $\approx$  5 -10%
- High number of doubtful cases makes frequent the need of biopsies
- Conventional mammography is **not enough effective** for dense breasts

*Radiographs of breasts with increasing density: mainly adipose breast (left) up to high fibro-glandularity breast (right)*



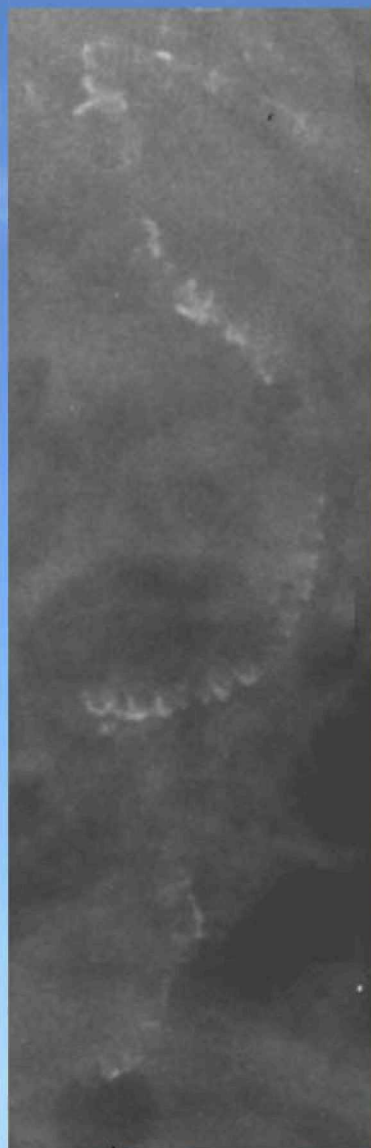
Breast composition and its mammographic appearance.<sup>1</sup>

# PHC application to mammography: Human tissue sample



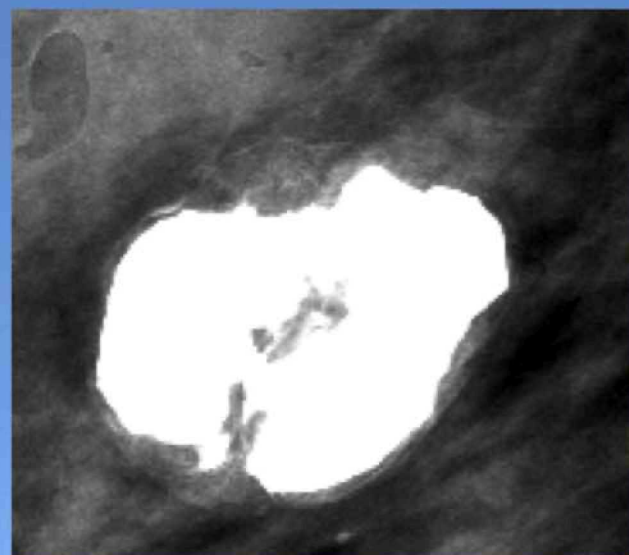
E = 17 keV

SR



Conventional X-ray generator

30 kVp, 50 mAs

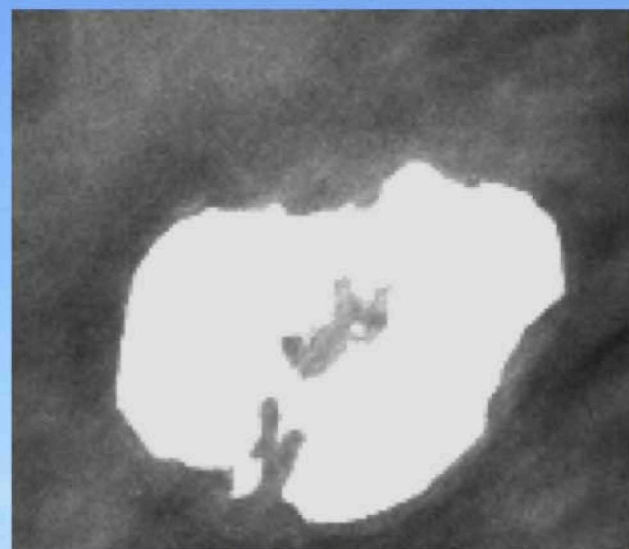


SR

E = 17 keV



Thickness = 4 cm  
MGD = 1.5 mGy



## The SYRMA project (**SY**nchrotron **R**adiation for **MA**mmography)

*Agreement among the Public Hospital of Trieste, the University of Trieste and Elettra*

Aim -> *In vivo* mammography studies on cases selected by the Radiologist.

Target-> Dense breasts;

conventional radiographs with uncertain diagnosis;

suspect of false positives.

Set-ups-> I Phase: PHC radiography with commercial detectors;

II Phase: low-dose tomography with custom Si microstrip detector.

**Clinical trial started on March 13, 2006**

# Patients' selection

---

The patient recruitment is performed on the basis of the BI-RADS classes of the American College of Radiology (recognized by the European Guidelines for breast screening). A patient is a candidate suited to SR:

- When mammography shows a dense disomogeneous breast and ultrasonography does not solve the problem - Class R1
- When mammography shows an asymmetry of the two breasts, not understood by ultrasonography - Class R3
- When both mammography and ultrasonography are uncertain - Class R3 and R4.

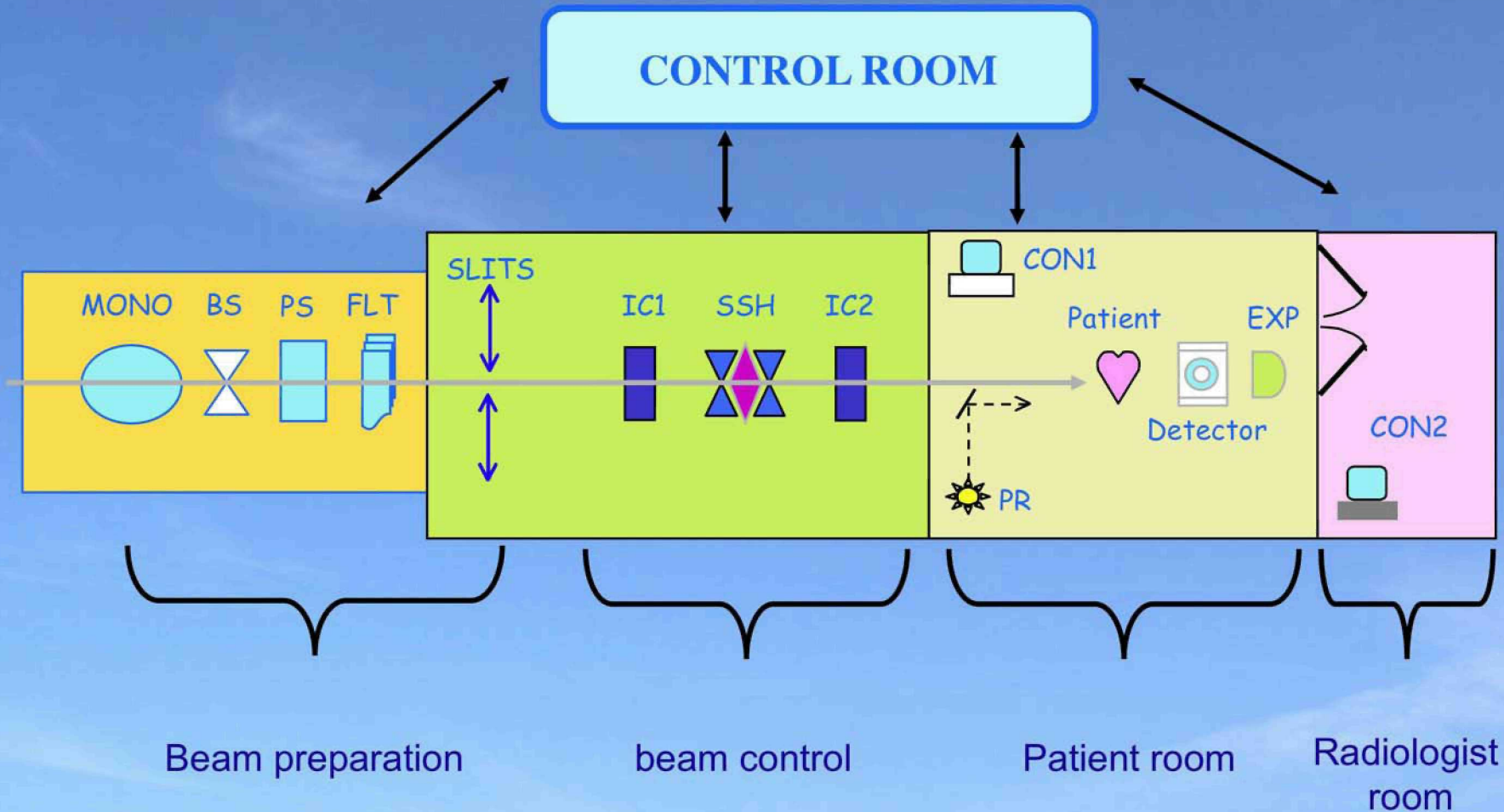
## **Methods used for comparing SR vs. conventional images**

Better lesions characterization

Enhanced visibility of microcalcifications

Detectability of new lesions

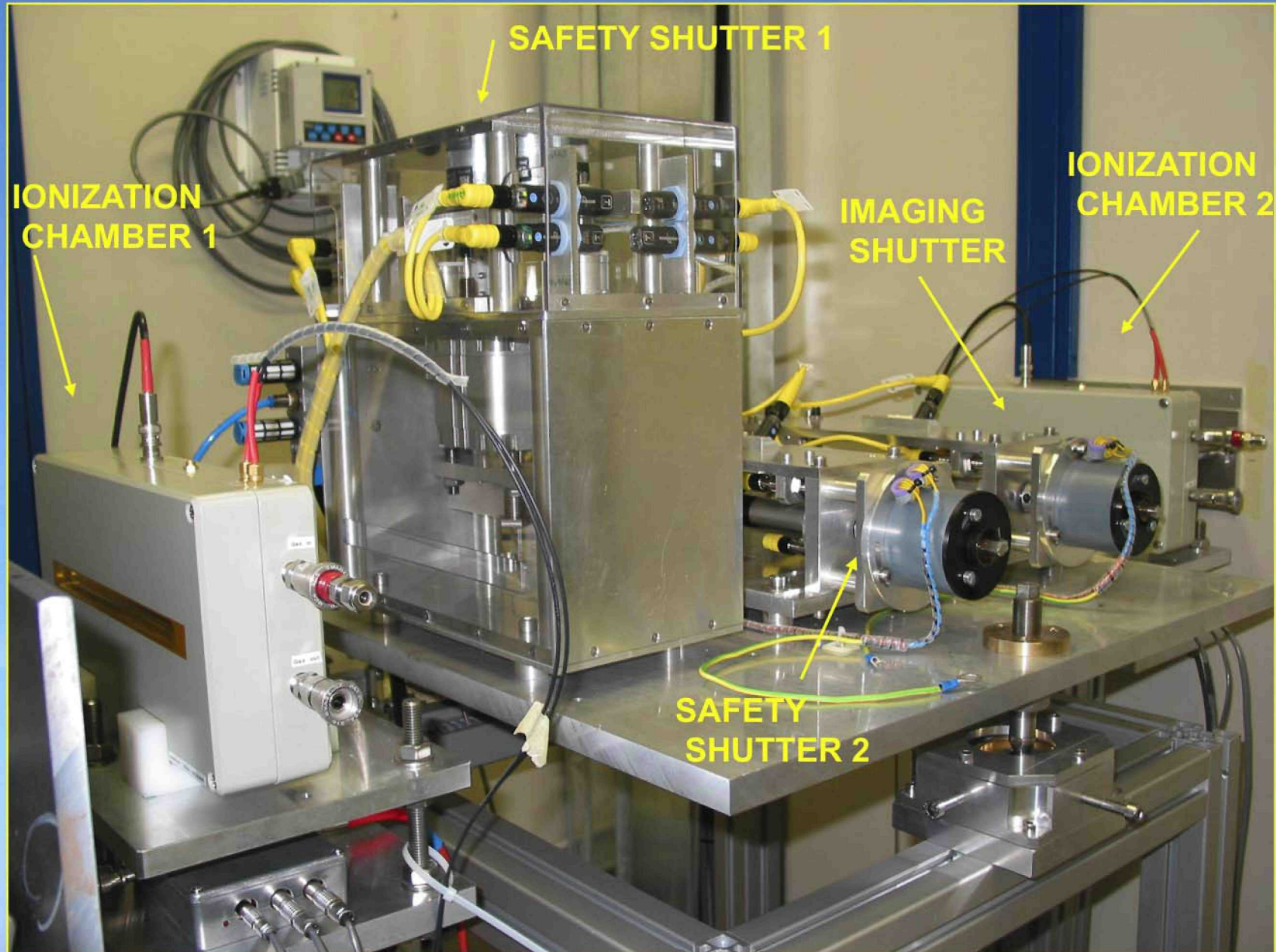
# The SYRMA beamline



## Safety systems:

- Beamline access control system (for personnel)
- Dose control system (for patient)

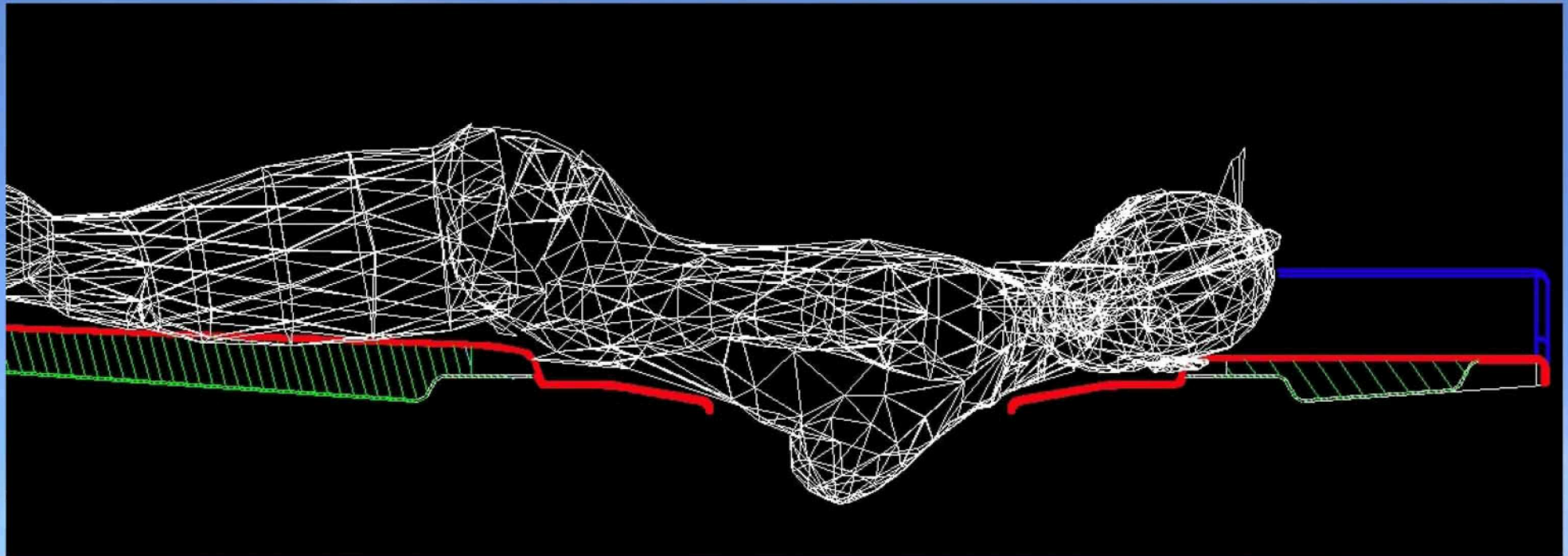
# Dose monitoring and shutters



# Radiologist room



# Patient positioning

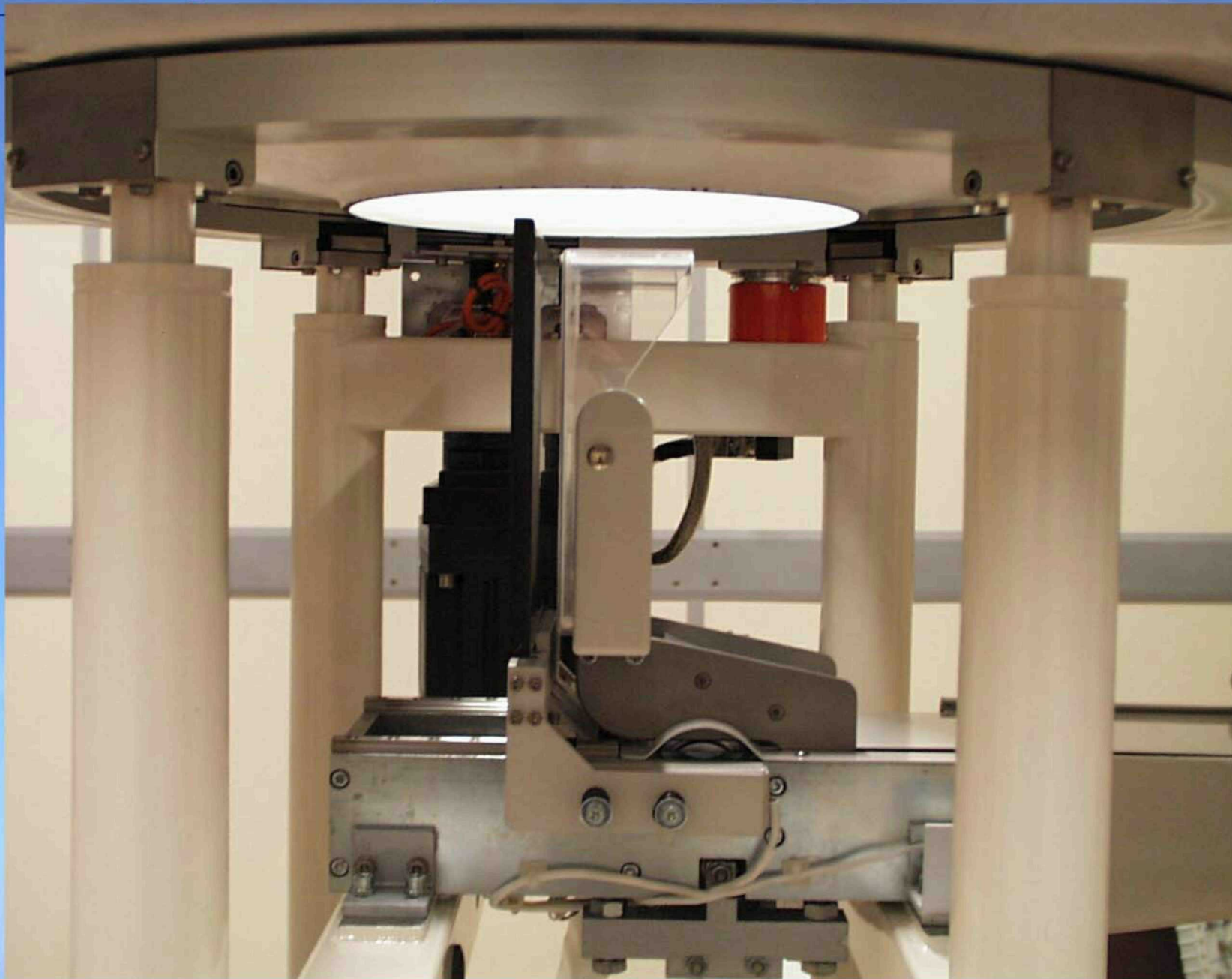




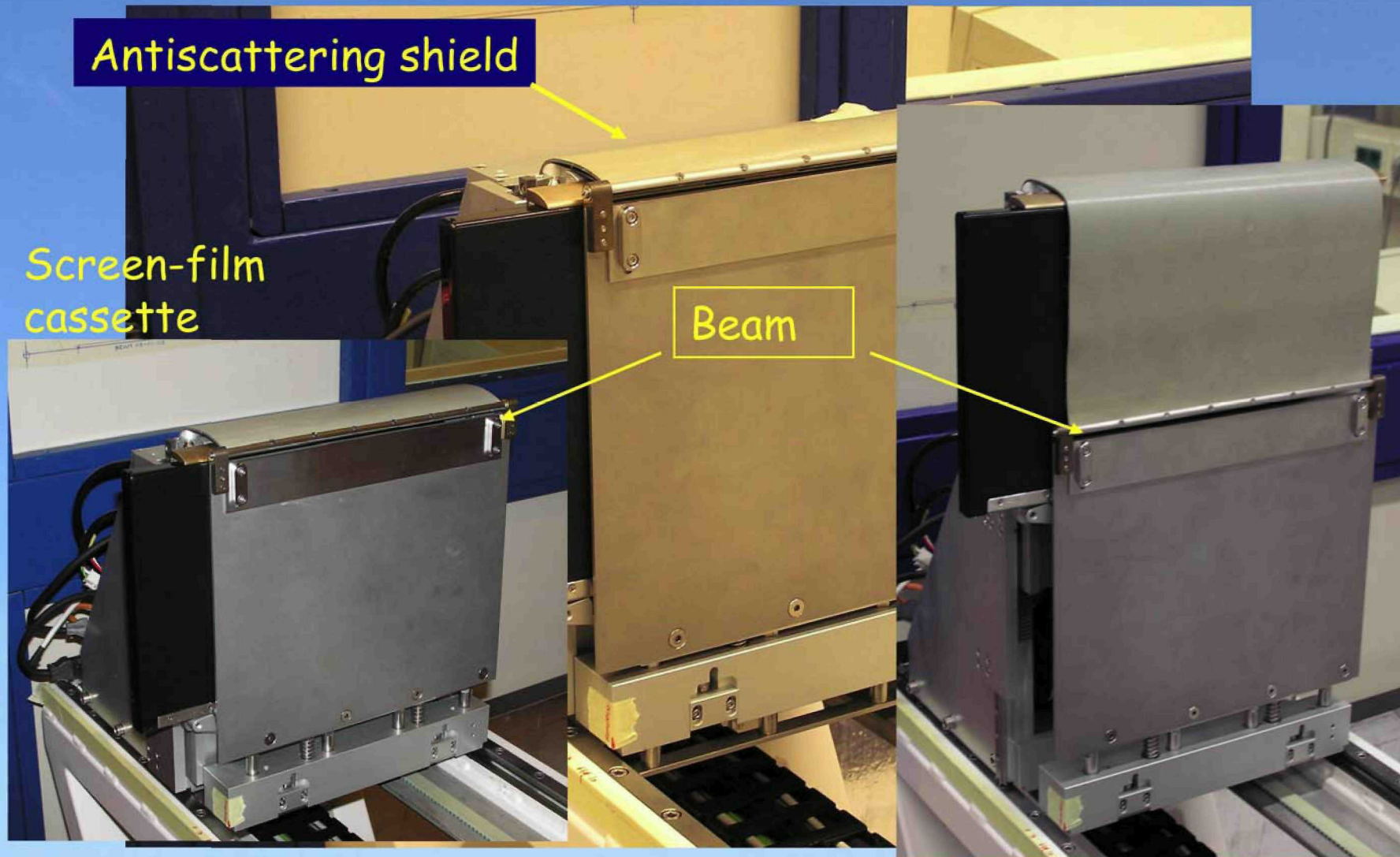
# Patient support



# Compression system



# Detector holder



## Procedures (controlled by examination Supervisor)

### *Exam initialization*

- Input of patient parameters,
- Choice of X-ray energy (according to the breast thickness and on an estimate of breast glandularity class (i.e. low, medium, high)),
- Beam optimization.

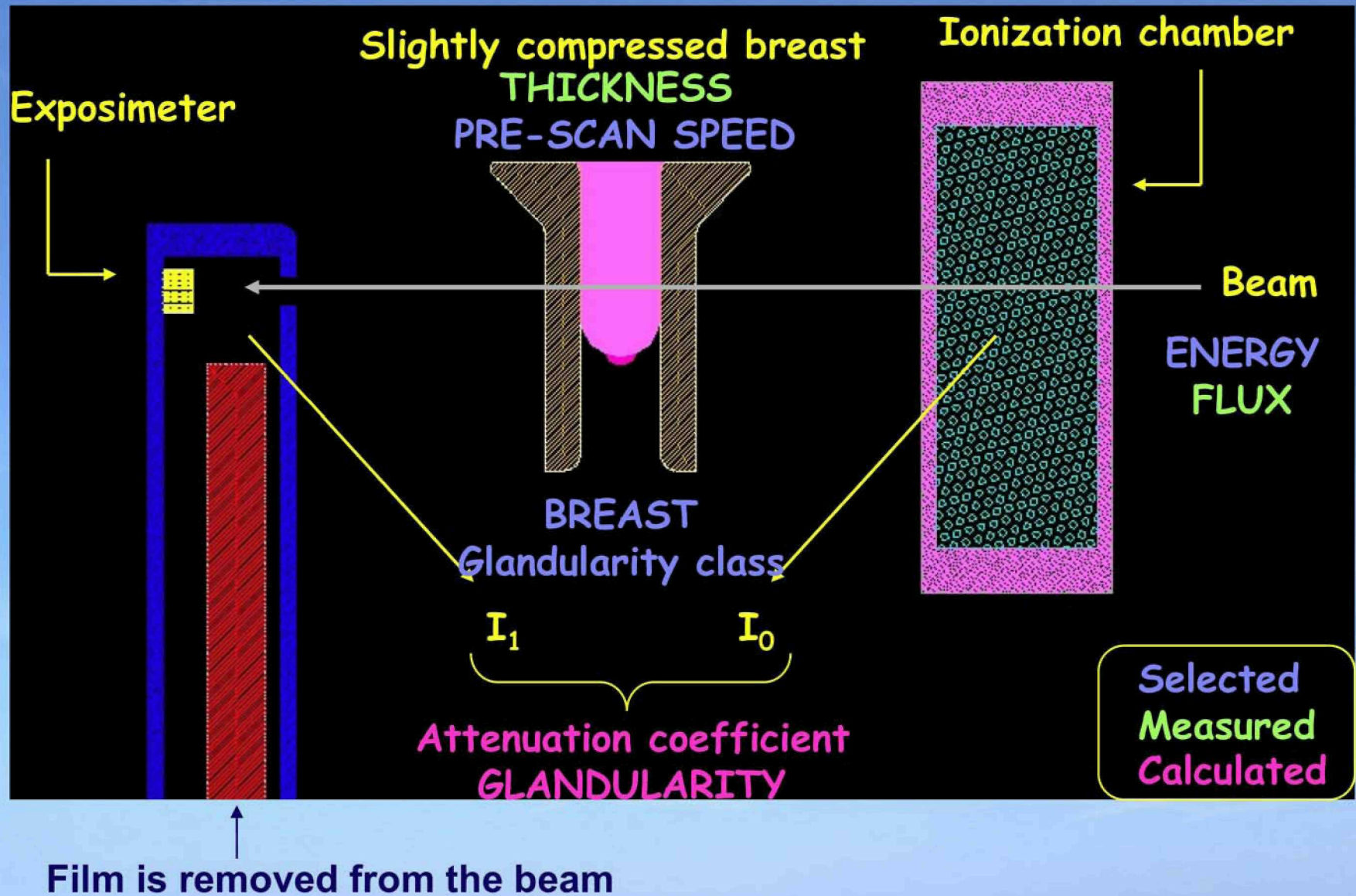
### *Prescan*

- It is a scan over a small breast portion in a range selected by radiologist.
- It aims to measure the breast absorption properties and to evaluate the real breast glandularity.
- The results of prescan are used to confirm the choice of the X-ray energy and to calculate the scan speed.
- The delivered dose is 5-10 % the examination dose.

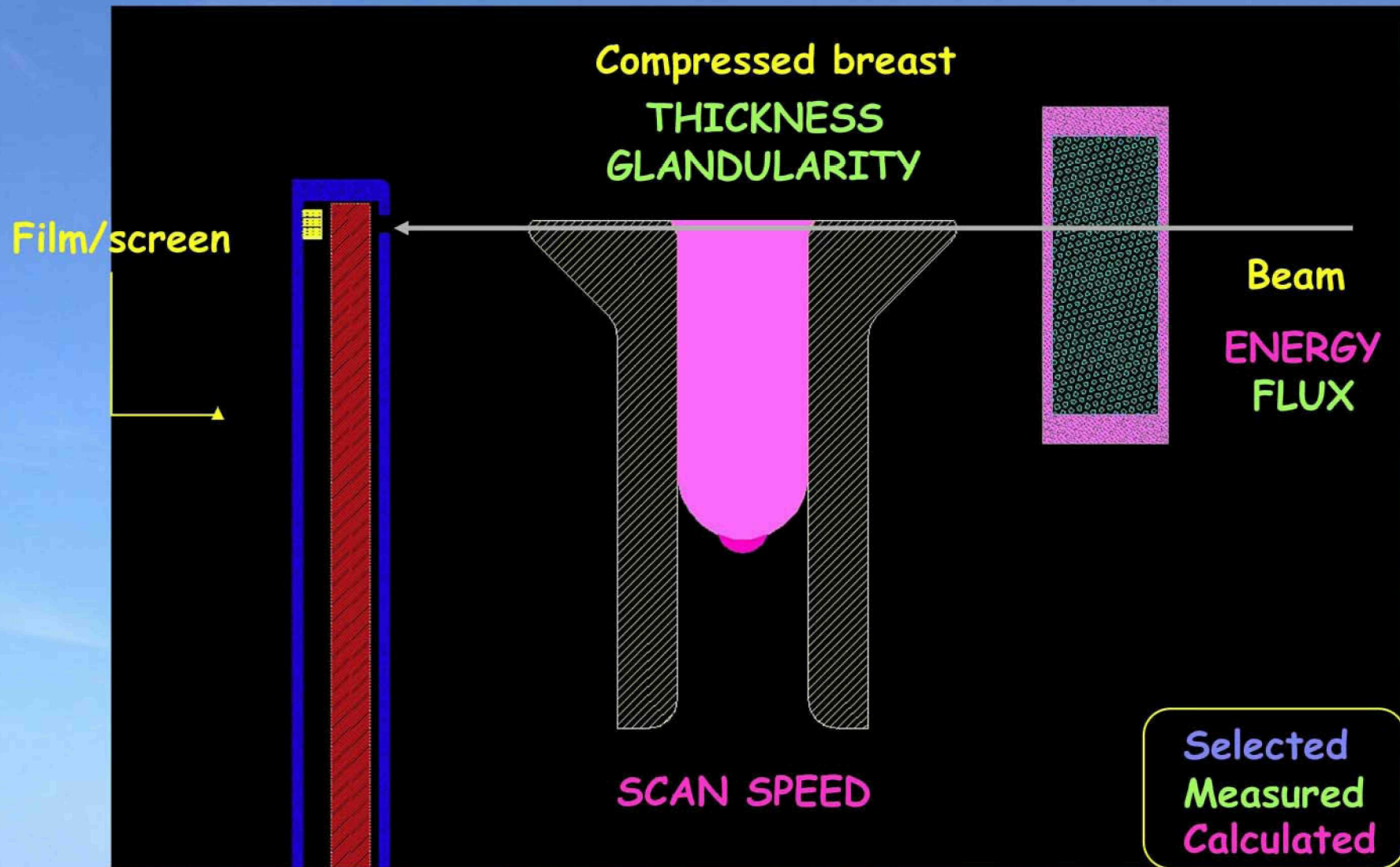
### *Exam*

- The exam is a simultaneous scan of breast and detector in a range selected by radiologist.

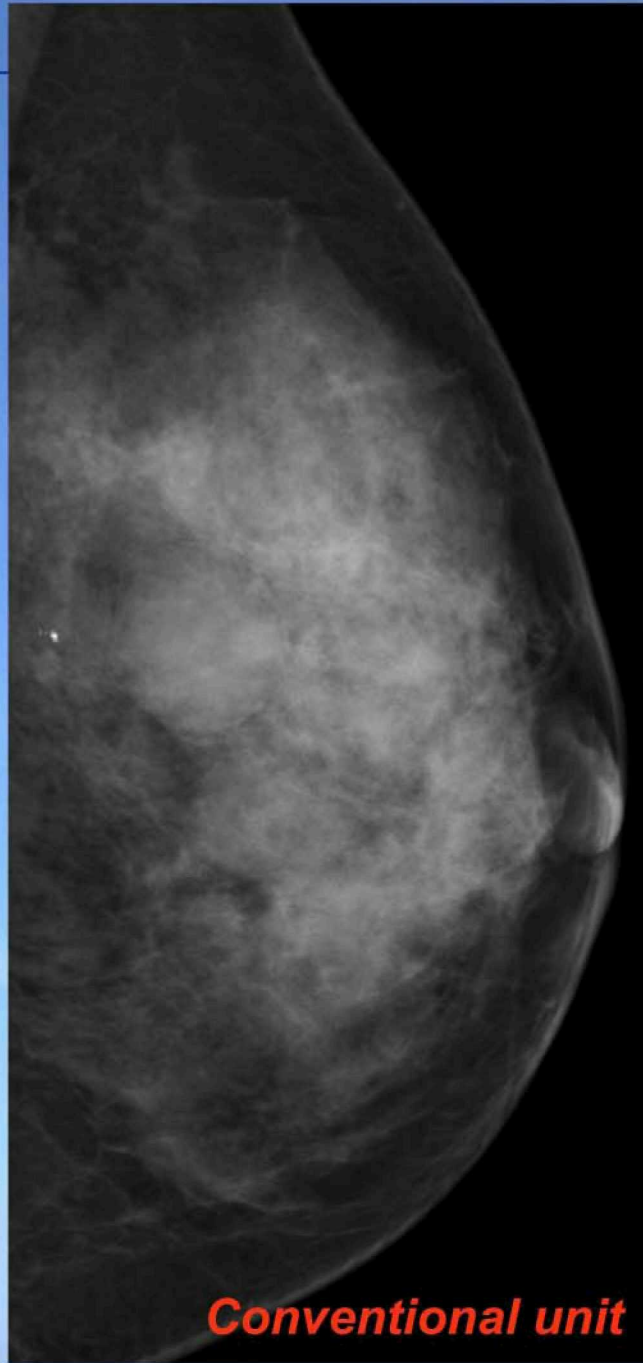
# Examination protocol: pre-exposure



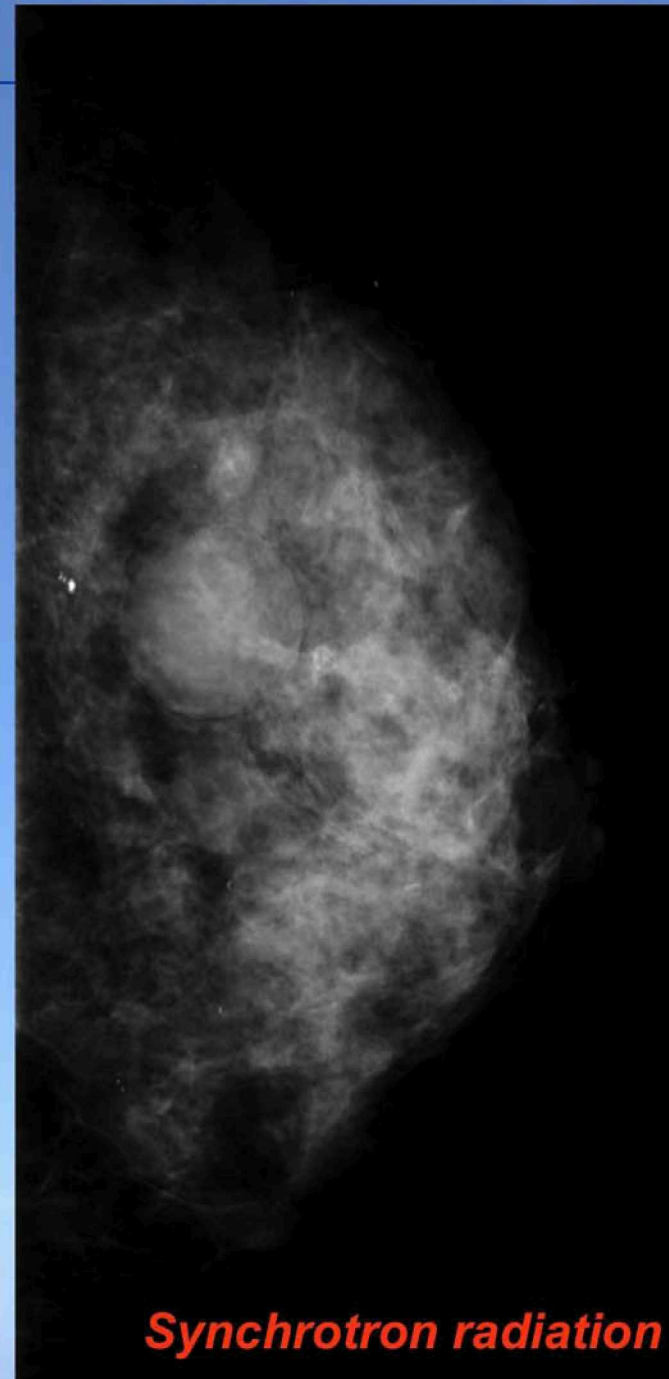
# Examination protocol: exposure



Film in the beam



**Conventional unit**

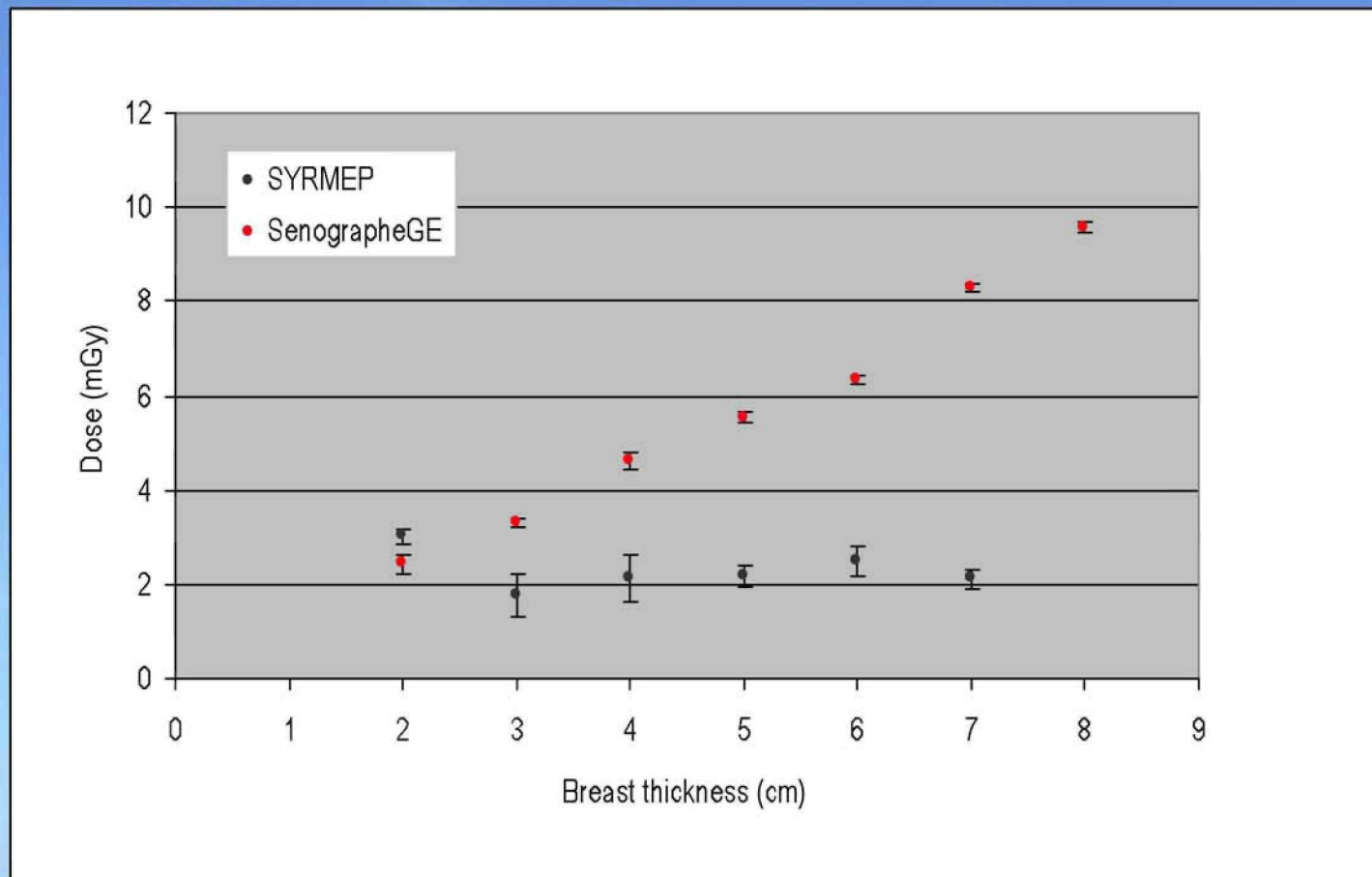


**Synchrotron radiation**

# Doses comparison I

Average Entrance Skin Doses delivered to patients at SYRMEP and at the conventional mammographic unit (Senographe GE)

Vertical bars indicate the data distribution of each thickness class

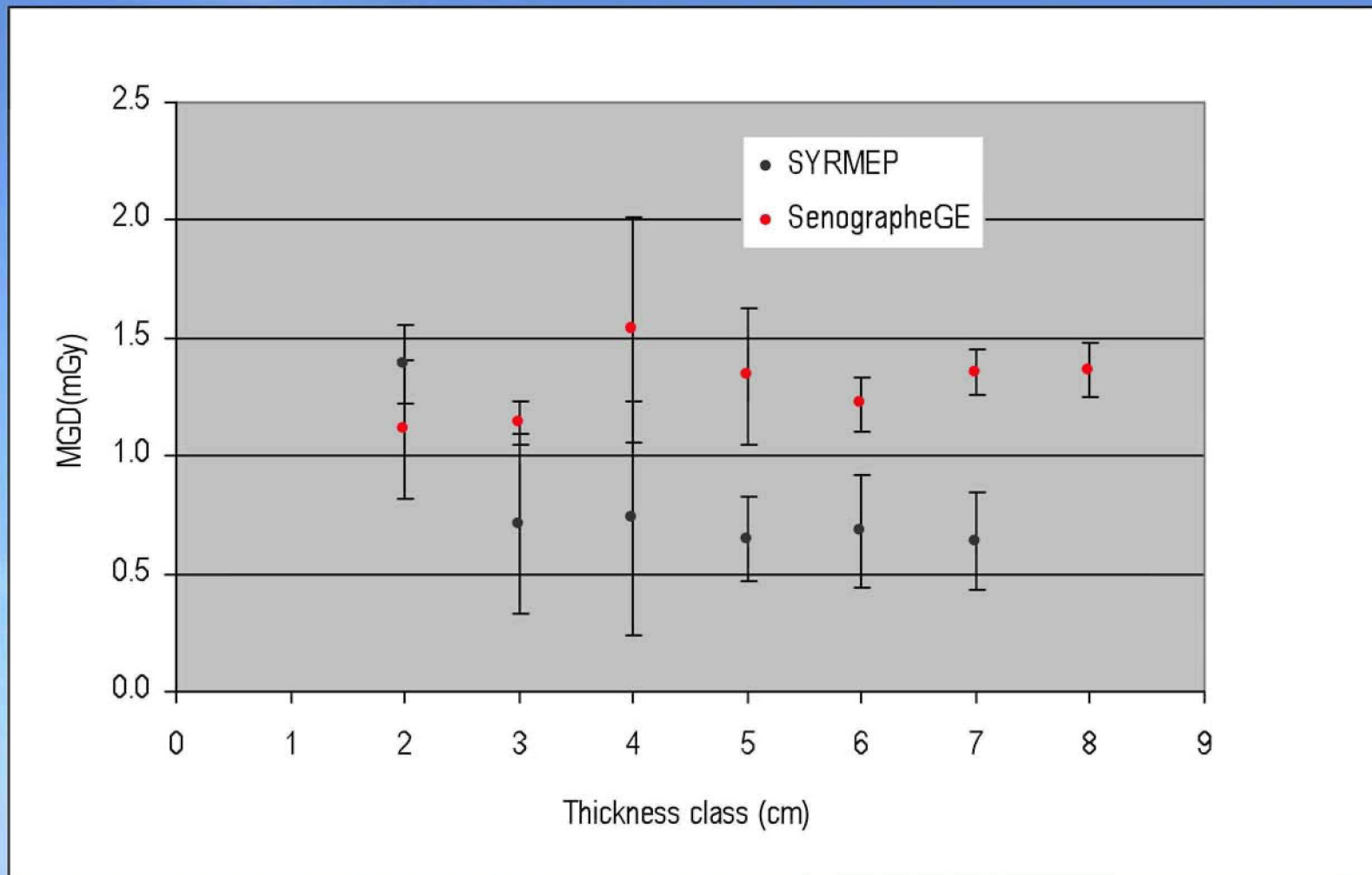




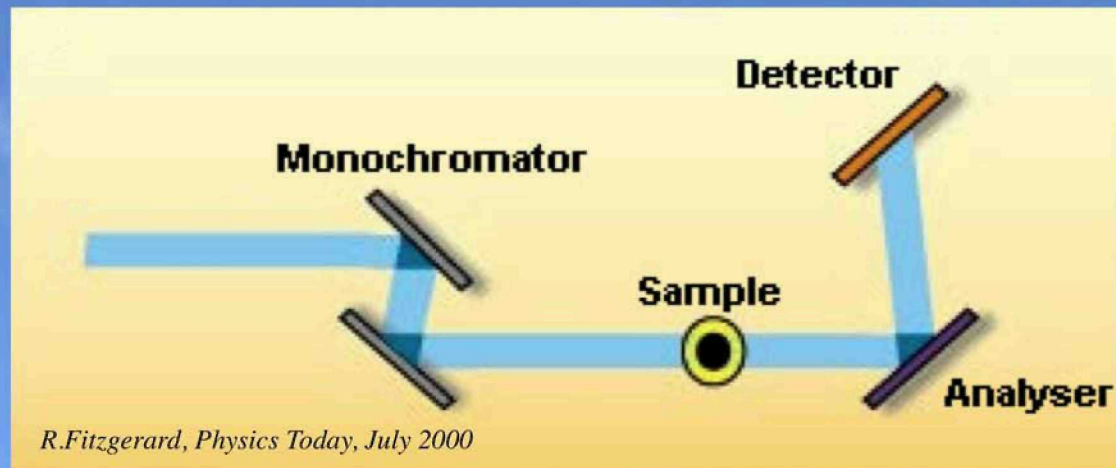
# Doses comparison II

Average Mean Glandular Doses delivered to patients at SYRMEP and at the conventional mammographic unit (Senographe GE)

Vertical bars indicate the data distribution of each thickness class

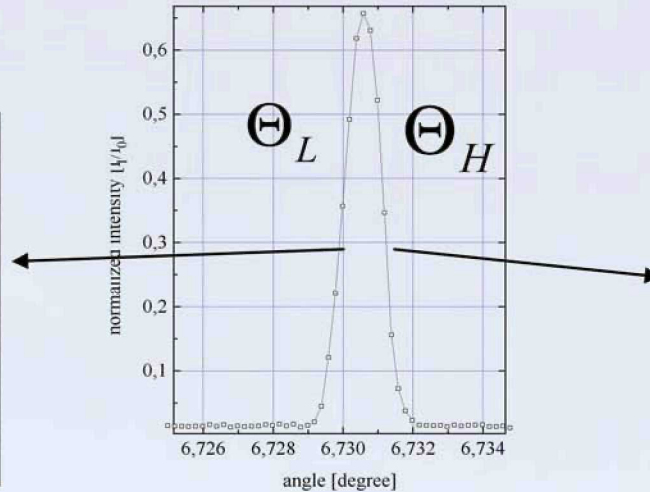
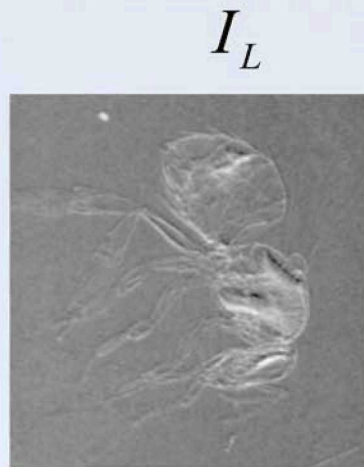


# Diffraction Enhanced Imaging (DEI)



- A perfect crystal, positioned between sample and detector, is used as an angular filter to select angular emission of X-rays. The filtering function is the rocking curve (FWHM: 1-20  $\mu\text{rad}$ )
- Image formation with DEI is sensitive to a variation of  $\delta$  in the sample. Indeed, **refraction angle is roughly proportional to the gradient of  $\delta$**
- Analyzer and monochromator aligned  $\rightarrow$  X-ray scattered by more than some tens  $\mu\text{rad}$  are rejected
- Small misalignments  $\rightarrow$  investigation of phase shift effects
- With greater misalignments the primary beam is almost totally rejected and pure refraction images are obtained
- Sensitive to  $\nabla\Phi(x,y)$

# DEI image manipulation (Original Algorithm)

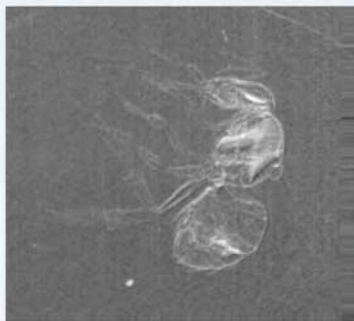


$$I_L = I_R \left( R(\Theta_L) + \frac{\partial R}{\partial \Theta}(\Theta_L) \Delta \Theta_z \right)$$

$$I_H = I_R \left( R(\Theta_H) + \frac{\partial R}{\partial \Theta}(\Theta_H) \Delta \Theta_z \right)$$

$\Theta_z$  = refraction Image

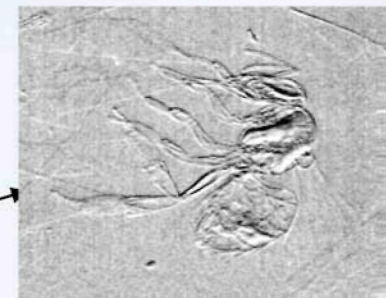
$I_R$  = apparent absorption image (absorption + extinction)



Apparent Absorption Image

$$I_R = \frac{I_L \cdot \frac{dR}{d\Theta} \Big|_{\Theta_H} - I_H \cdot \frac{dR}{d\Theta} \Big|_{\Theta_L}}{R(\Theta_L) \cdot \frac{dR}{d\Theta} \Big|_{\Theta_H} - R(\Theta_H) \cdot \frac{dR}{d\Theta} \Big|_{\Theta_L}}$$

$$\Theta_z = \frac{I_H \cdot R(\Theta_L) - I_L \cdot R(\Theta_H)}{I_L \cdot \frac{dR}{d\Theta} \Big|_{\Theta_H} - I_H \cdot \frac{dR}{d\Theta} \Big|_{\Theta_L}}$$



Refraction Image

# III

## Studies of cartilages and joints

Technique: DEI

Image modality: planar

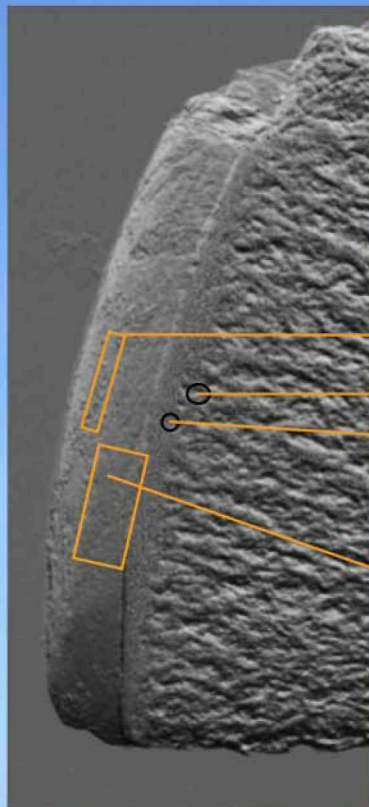
# Study on cartilage/bone interface

- Osteoarthritis (OA) is a disease characterized by the progressive degeneration of articular cartilage and the development of altered joint congruency.
- Incidence: 14% of the adult population.
- Conventional radiography detects only important osseous changes. Early changes in the cartilage and other articular tissues are not directly visible.
- Cartilage loss can only be indirectly inferred by the development of joint-space narrowing which can be highly unreliable, False positives: 20-40%.
- Need to monitorate: soft articular tissues, cartilages, early changes in the adjoining subchondral and trabecular bone. Articular cartilage and subchondral bone act in concert with regards to the mechanical loading of the joint.

# Study on cartilage/bone interface

Study of:

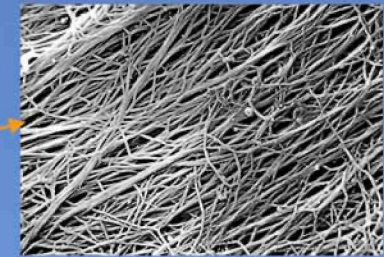
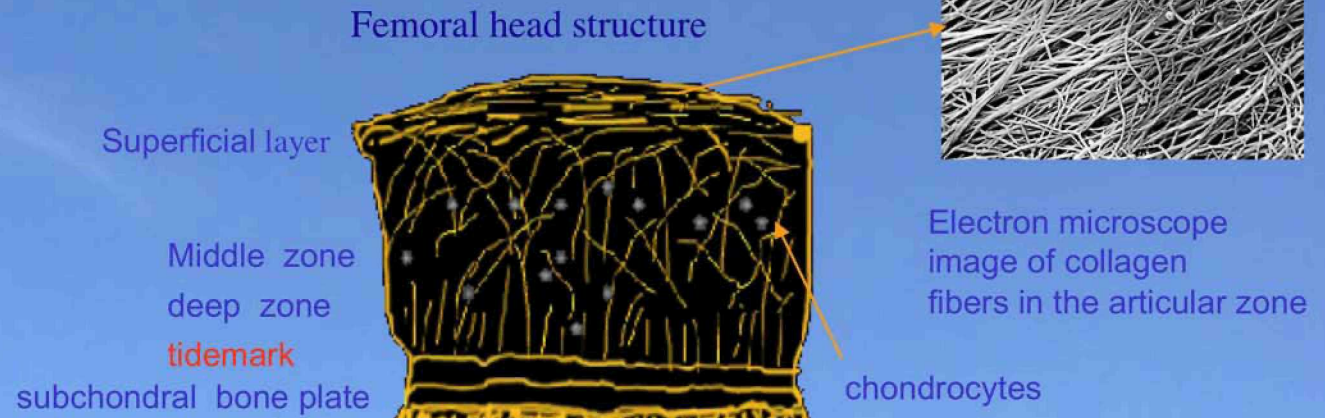
- cartilage
- cartilage bone interfaces
- changes in the bone structure



- Superficial Layer (Zone of horizontal collagen fibers with flat cells)
- Subchondral Bone Plate (**Important for diagnostic purposes in osteoarthritis**)
- Tidemark (Border between normal and mineralized cartilage)

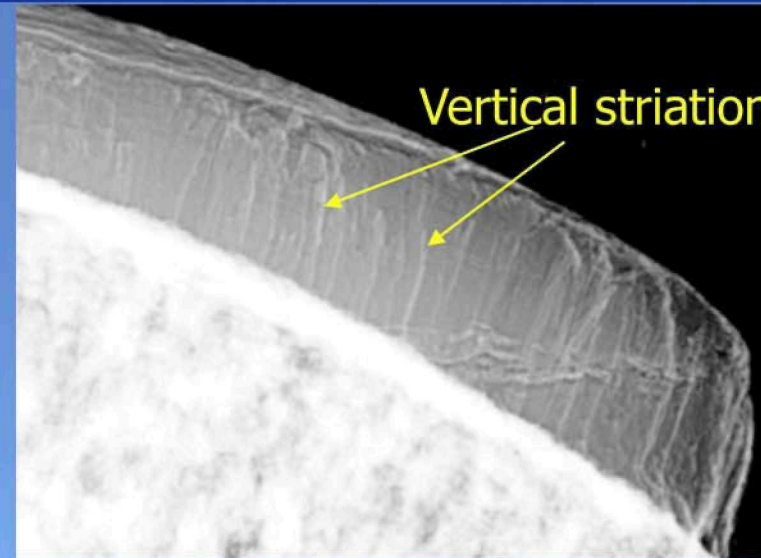
Transitional and Deep Layer (round cells, collagen fiber switches from horizontal to vertical orientation, increasing stiffness and material density)

Aim: detect the architectural arrangement of collagen within cartilage and evaluate how the cartilage degeneration affects the underlying subchondral and trabecular bone.

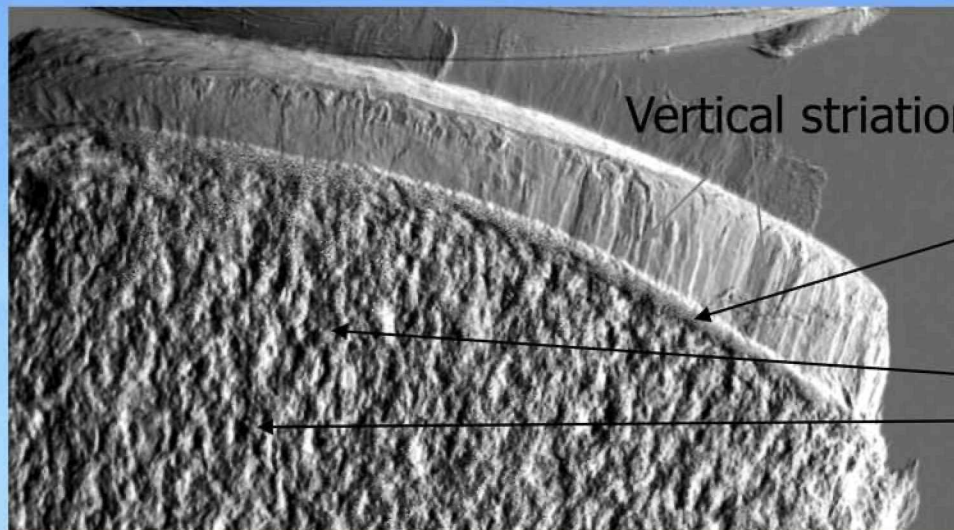


# Femur head core cuts: collagen arcades structure

- The DEI technique allows to visualize the discontinuities of the sample and the inner structures invisibles by means of conventional X-Ray imaging.
- The transition bone-cartilage is emphasized.
- The articular cartilage striations are well visible due to X-ray diffraction at edges of fibers



Refraction image



Apparent absorption image

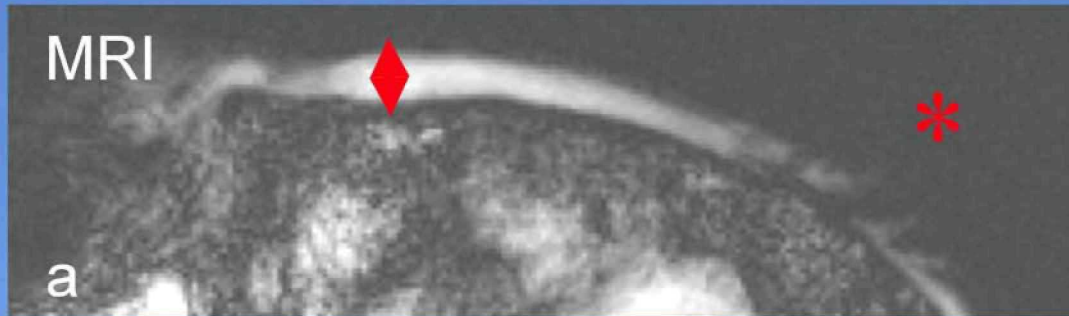
Elettra  
25 keV

Subchondral  
bone

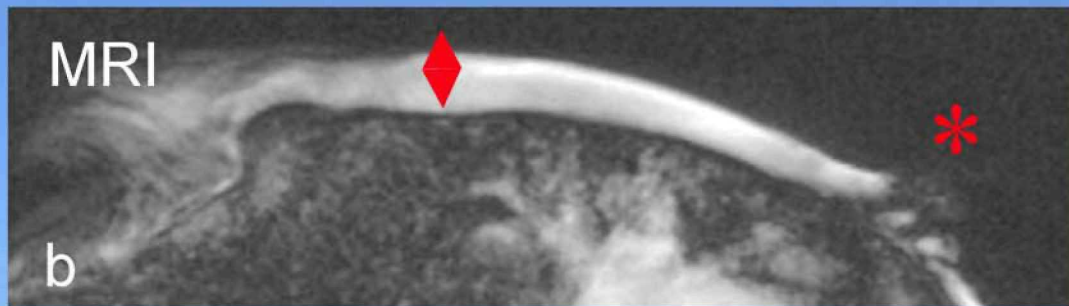
Trabecular bone

Muehleman C, Majumdar S, Issever AS, Arfelli F, Menk RH, Rigon L, Heitner G, Reime B, Metge J, Wagner A, Kuettner KE, Mollenhauer J, Osteoarthritis and Cartilage 12 (2): 97-105 FEB 2004

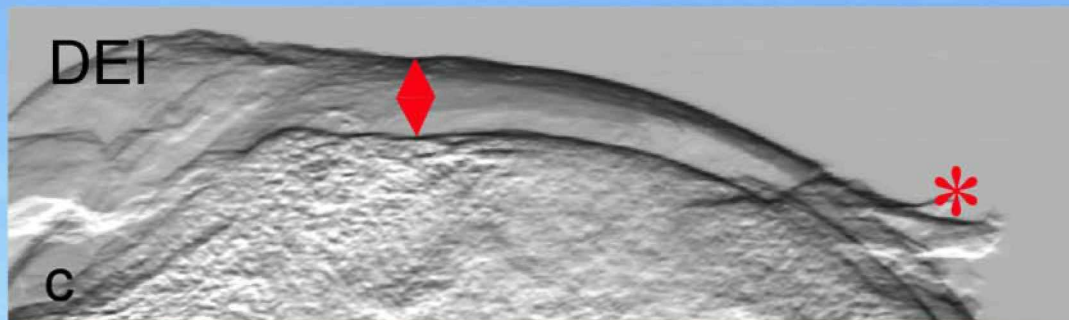
# Femur head core cuts: comparison with MRI



5 sec



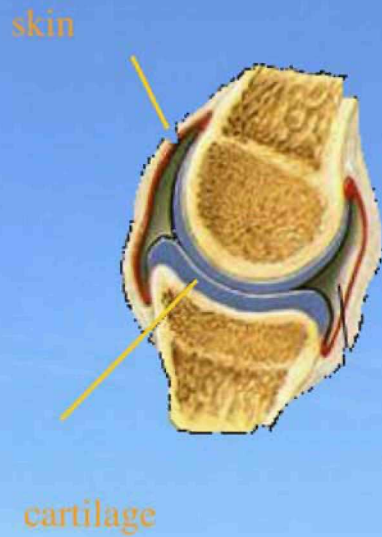
150 sec



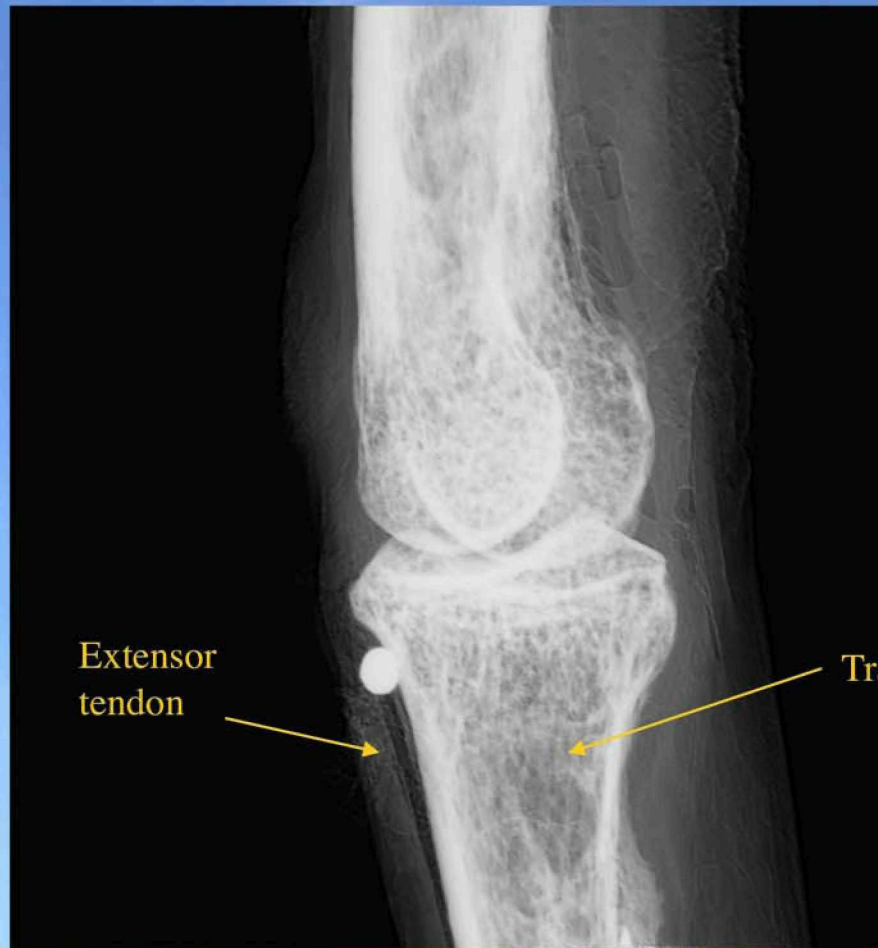
A Wagner, M Aurich, N Sieber, M Stoessel, WD Wetzler, K Schmuck, M Lohmann, B Reime, J Metge, P Coan, A Bravin, F Arfelli, L Rigon, RH Menk, G Heitner, T Irving, Z Zhong, C Muehleman, J A Mollenhauer submitted to NIM A



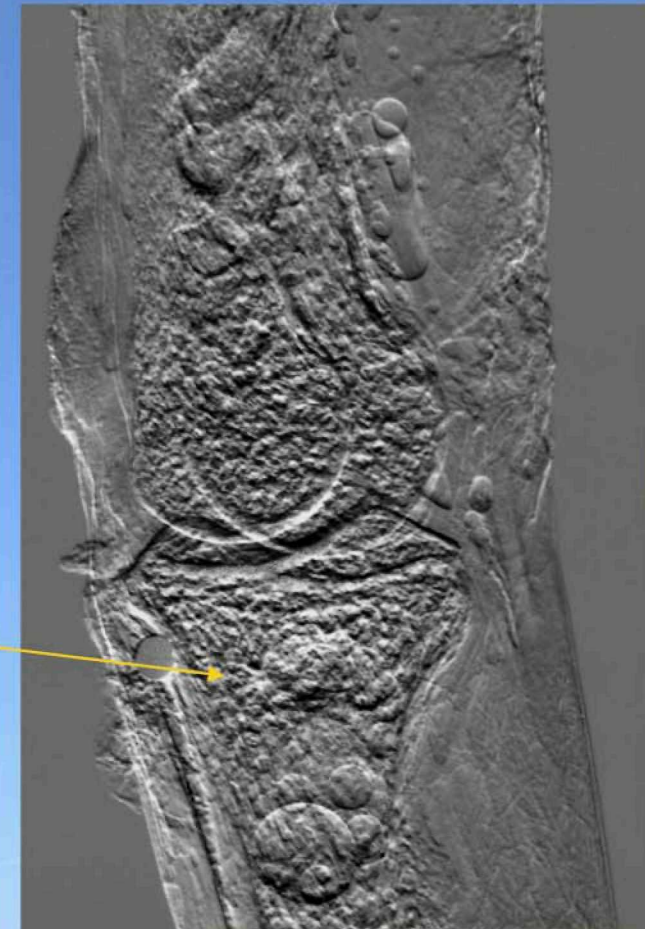
# Finger Joint



# Index finger proximal interphalangeal joint

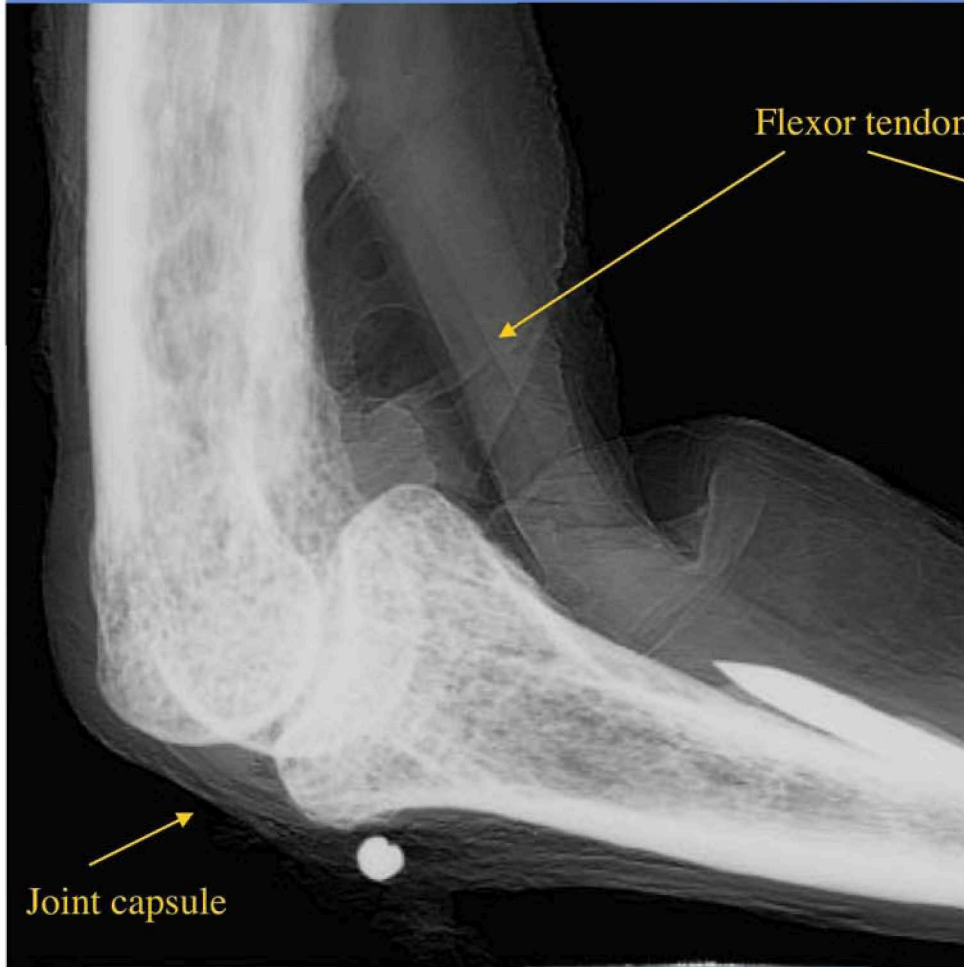


Apparent absorption Image

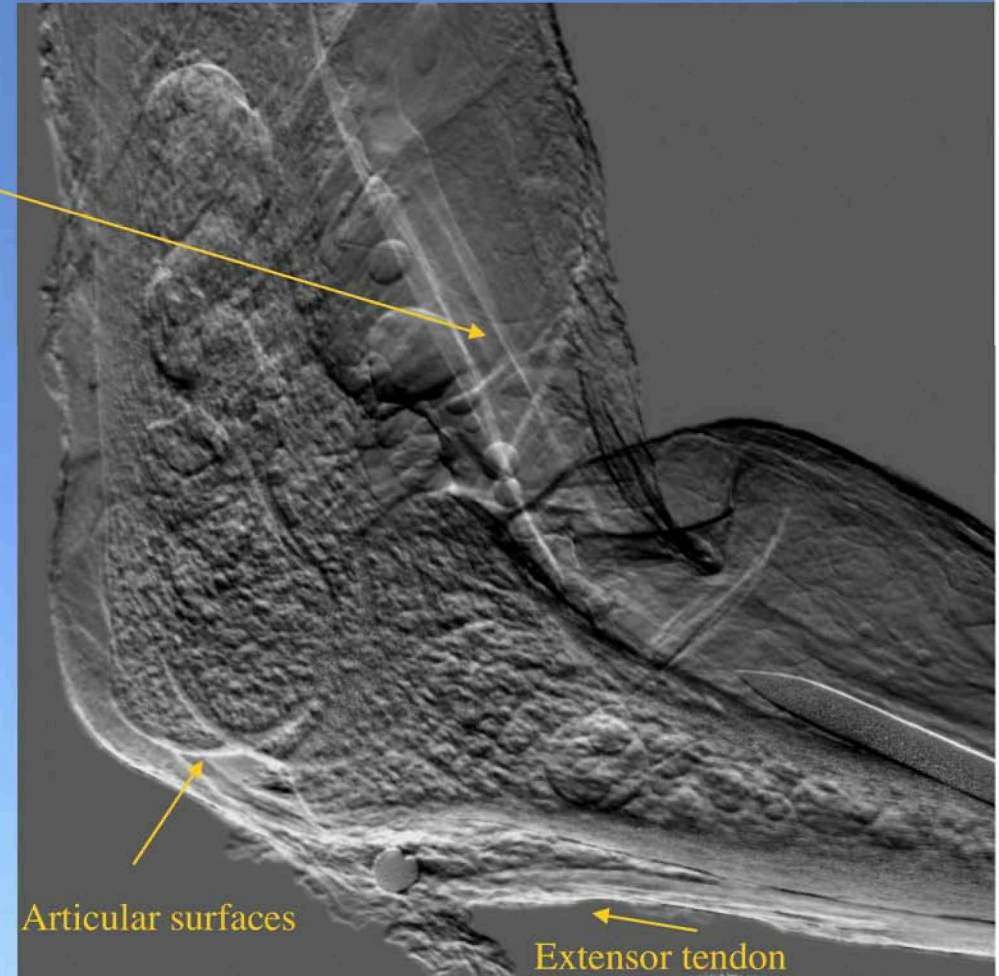


Refraction Image

# Index finger proximal interphalangeal joint



Apparent absorption Image



Refraction Image

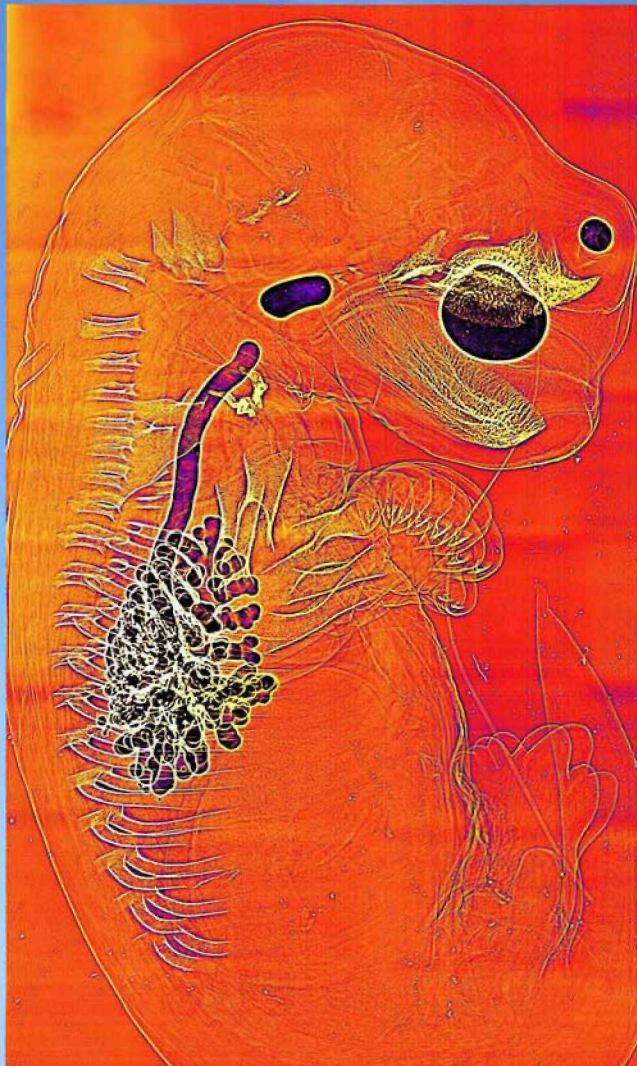
# IV

## Effects of Ventilation on Lung Liquid Clearance at Birth visualized by PHC Experience at SPRING-8

Technique:PHC

Image modality: planar

## Lung Liquid Clearance at Birth



Aeration of the lung and the transition to air-breathing at birth is fundamental to mammalian life.

It initiates major changes in cardiopulmonary physiology.

The dynamics of this process and the factors involved are largely unknown, because it has not been possible to observe or measure lung aeration on a breath-by-breath basis.

### **Birth: a major physiological challenge**

- Clear the airways of liquid
- Entry of air generates surface tension
- Separation of the pulmonary and systemic circulations
- 10 fold increase in pulmonary blood flow
- Large increase in blood oxygenation

## Lung Aeration in Preterm infants:

Can suffer from:

- Airway liquid retention → respiratory insufficiency
- Non-uniform ventilation → lung injury
- Delayed/blunted physiological transformation

It has not been possible to observe or measure lung aeration

- **Enter Phase Contrast X-ray Imaging!**

## Imaging lung aeration from birth

- Animal model: rabbit pups
- Imaged pups with PHC at SPring-8, Japan (Beamline 20B2).
  - Either before the first breath (fetus) or at fixed intervals after birth (up to 2h)



Absorption Contrast



Phase Contrast, 25 keV,  $z=2$  m

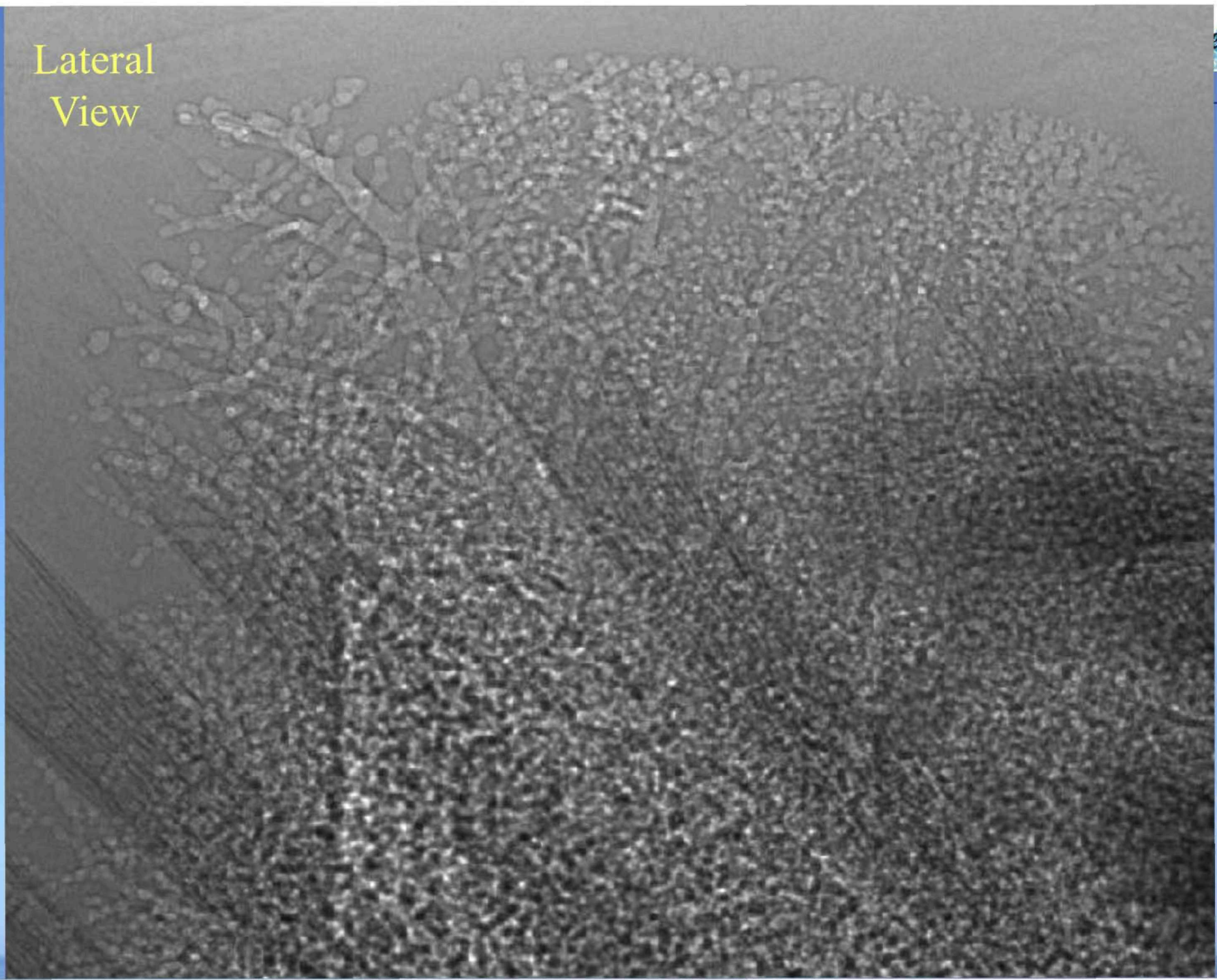




Imaging the terminal airways



# Lateral View



# Acknowledgement

---

to the SYRMEP/SYRMA team:

A.Abrami, V.Chenda, D.Dreossi, L.Mancini, E.Quai, R.H. Menk,  
N.Sodini, F.Zanini  
*Sincrotrone Trieste*

F.Arfeffi, E.Castelli, R.Longo, L.Rigon  
*University and INFN Trieste*

P.Bregant, M.Cova, E.Quaia, D.Sanabor, M.Tonutti, F.Zanconati  
*Radiology Dept. and Health Physics – University and Cattinara  
Hospital Trieste*

---

V

# Studies of human aortas

Technique: PHC

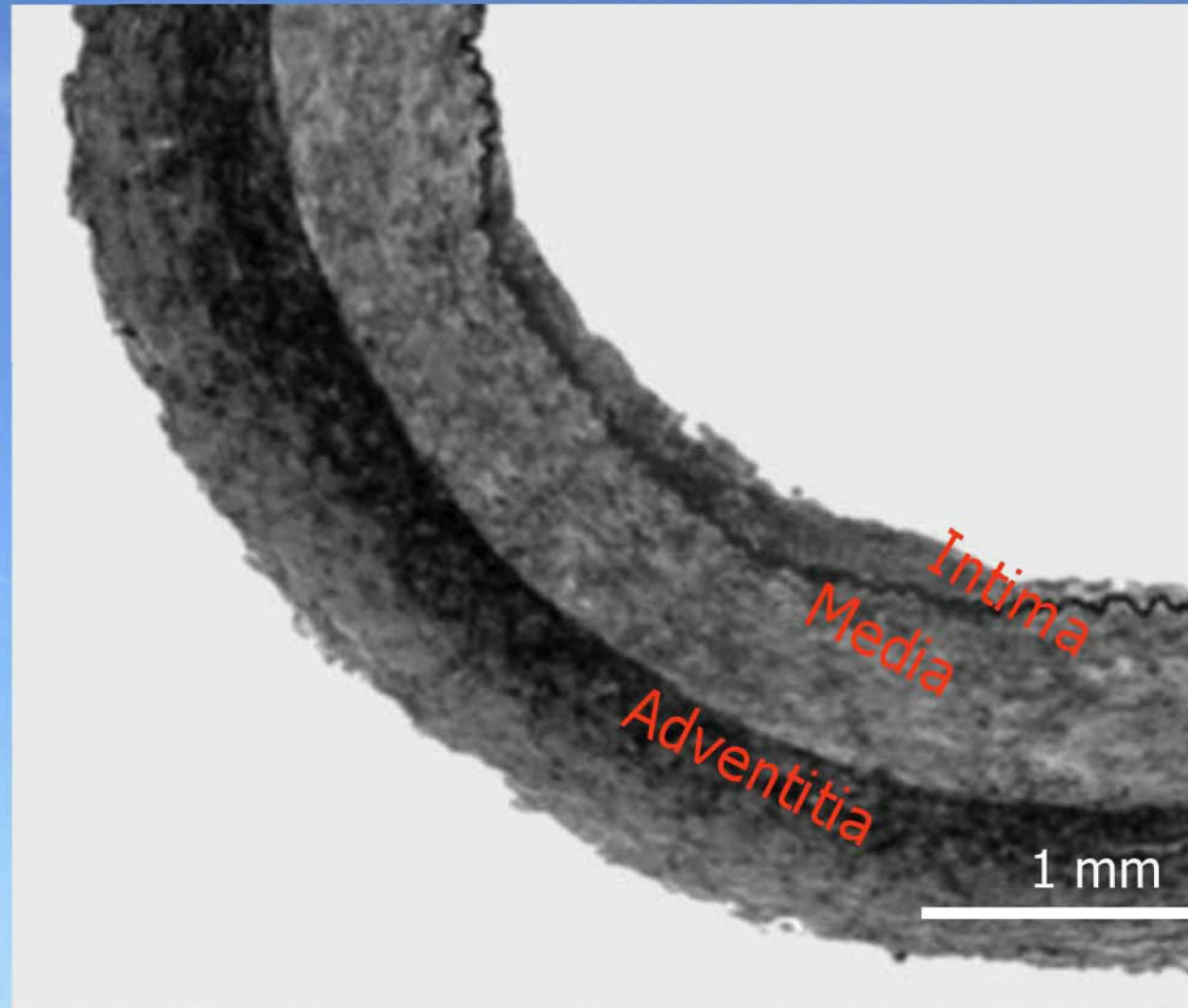
Image modality: micro-CT

# Micro-tomography of human aortas

---

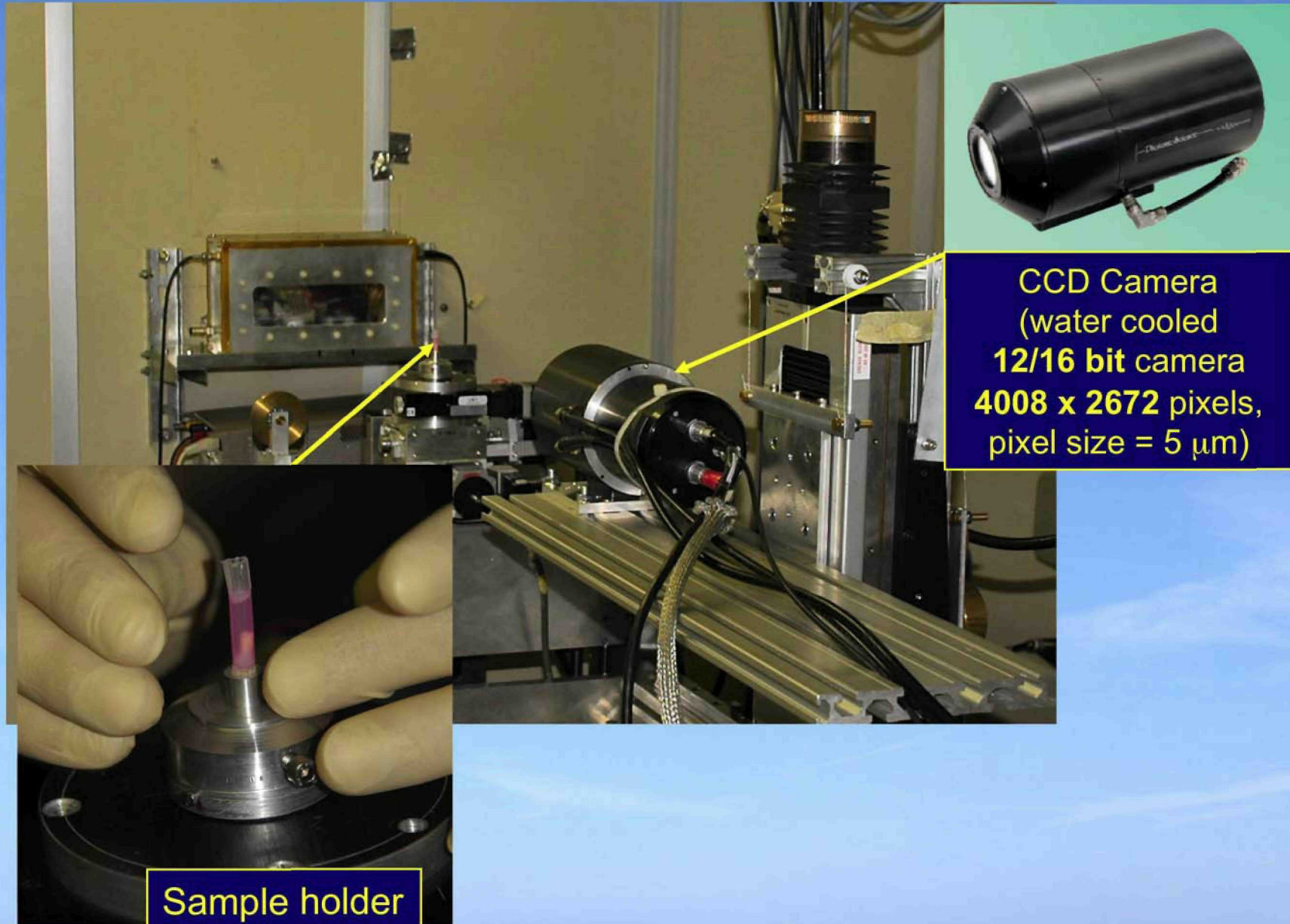
## *In situ* characterization of atherosclerotic plaques

- The investigation of the arterial wall is an essential issue for the early diagnosis of atherosclerosis
- Aim of the feasibility study at SYRMEP: reveal the different layers and plaques components of diseased arteries.
- Final aim: generate **morphological models** for finite element analysis codes applied for stress-strain analysis of arteries. **Bio-mechanical properties** are studied by SAXS. These codes allow to simulate arterial walls behavior during medical interventions such as balloon angioplasty.
- At present hrMR images are used but tissue differentiation is poor. Can we improve it using SR?



Cross section of a human artery

# SYRMEP: Micro-tomography set-up

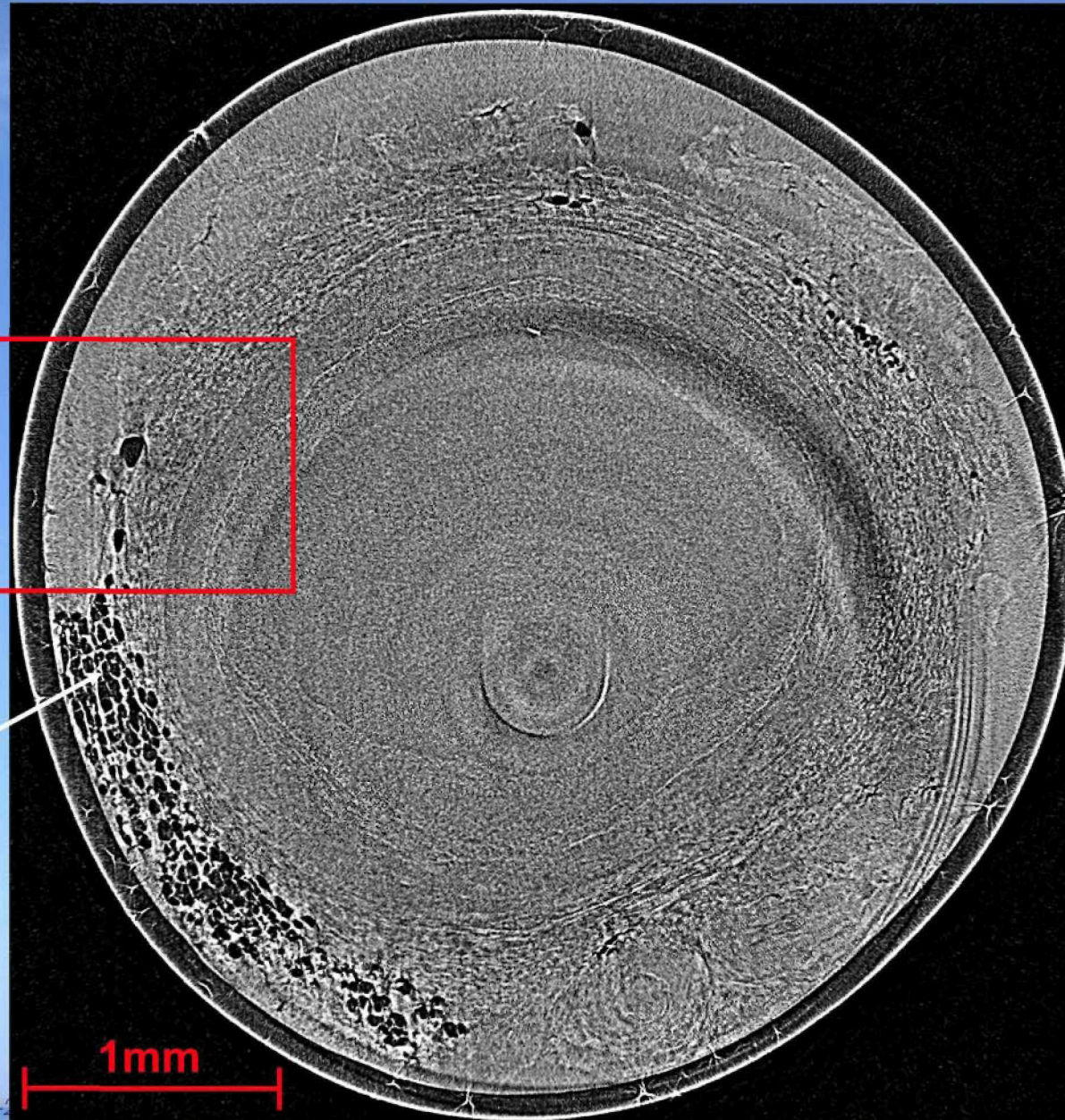


CCD Camera  
(water cooled  
**12/16 bit** camera  
**4008 x 2672** pixels,  
pixel size = 5  $\mu\text{m}$ )

Sample holder

# Aged non-diseased coronary vessel

Slice

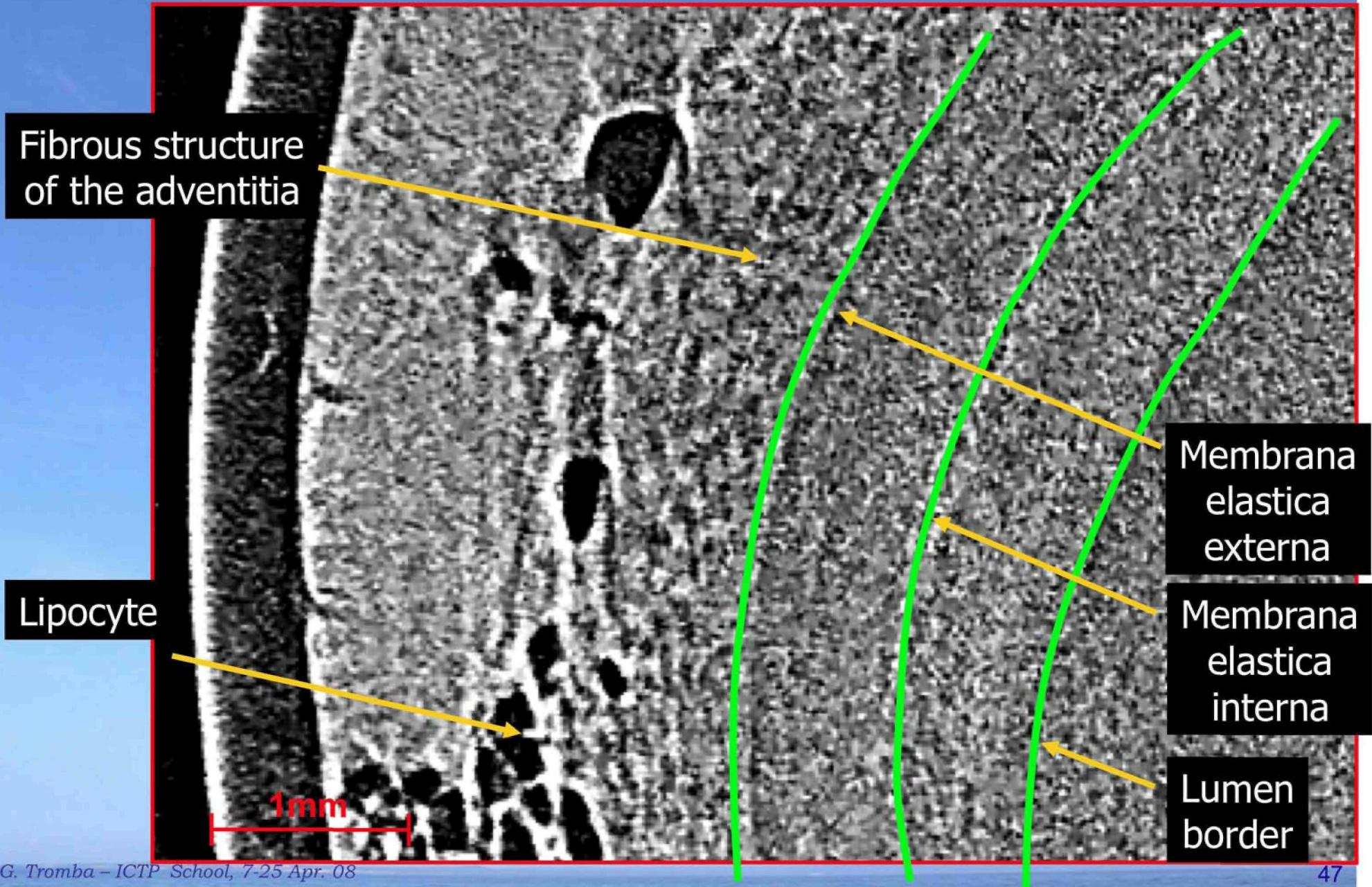


Lipocytes  
(fat cells)

1mm

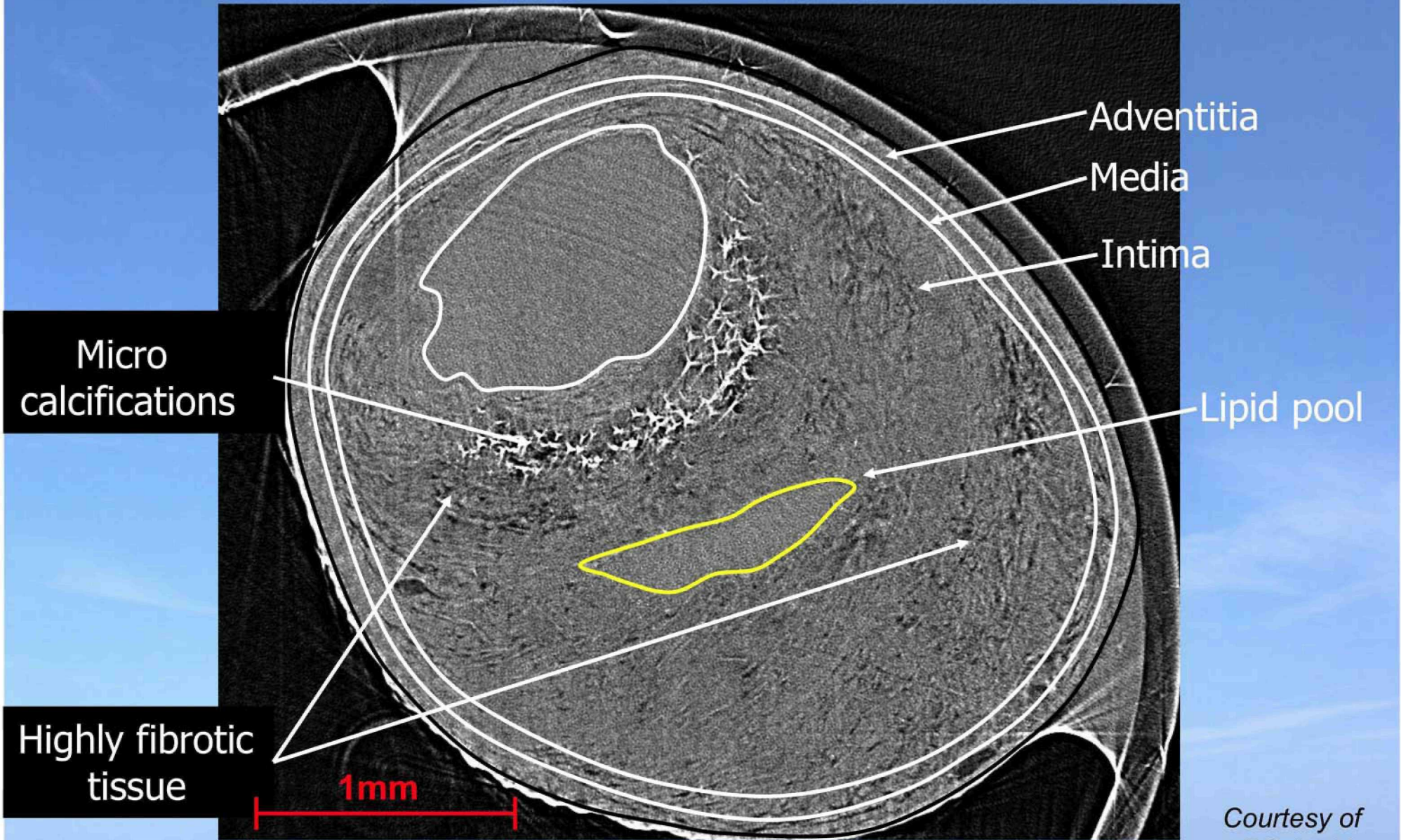
Courtesy of  
F.Schmid

# Aged non-diseased coronary vessel



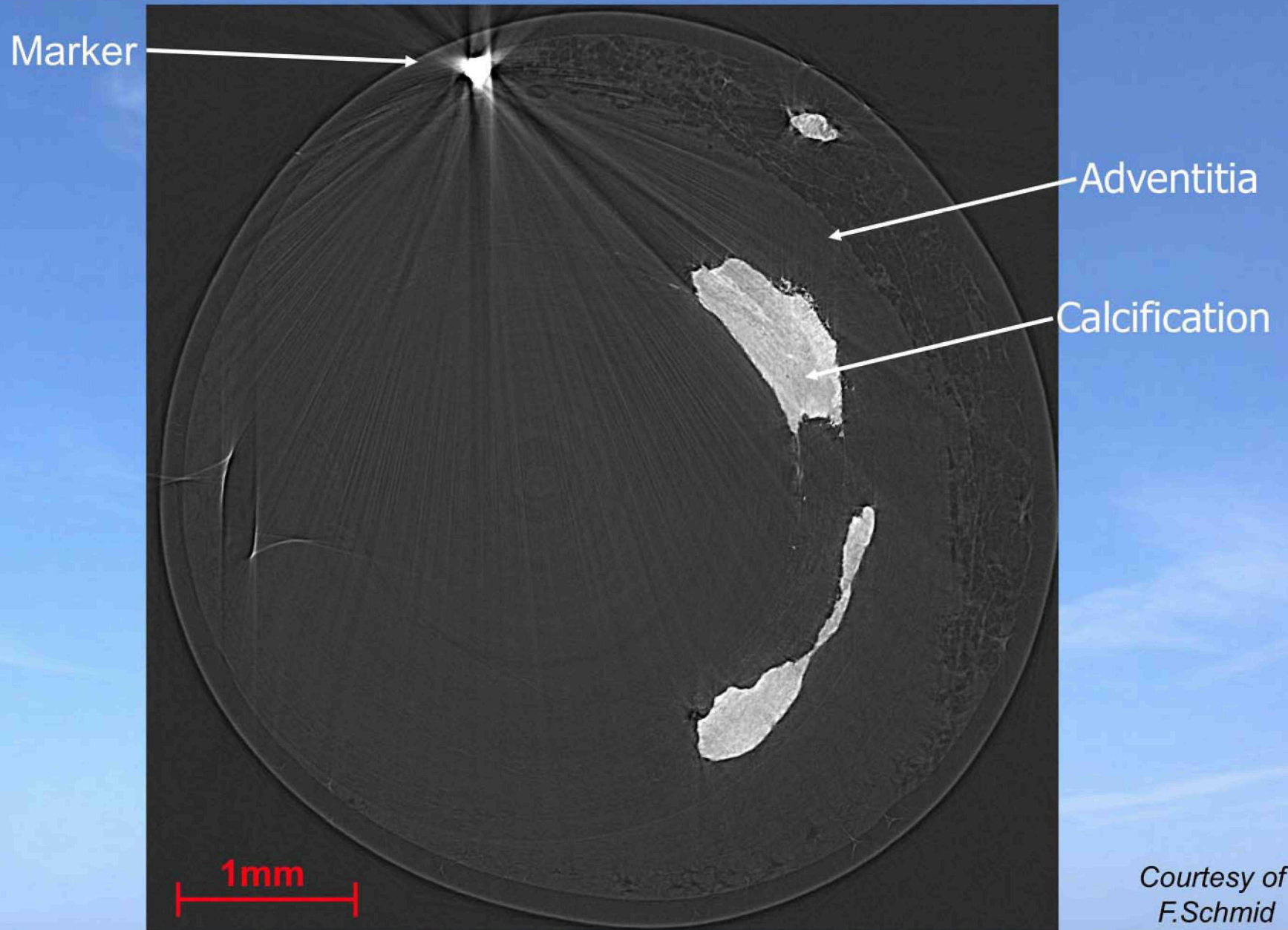


# Aged diseased coronary vessel

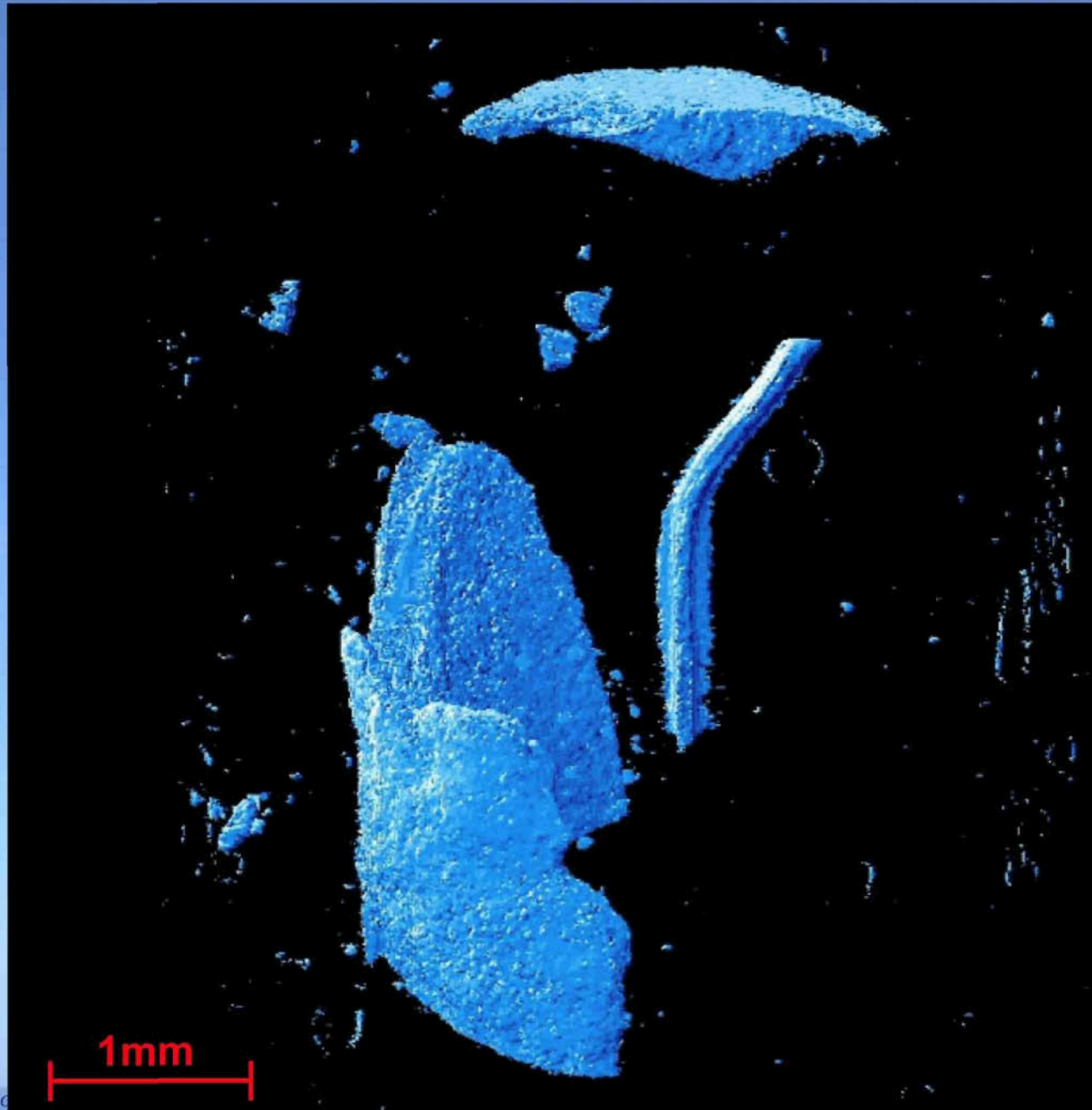


Courtesy of F.Schmid

# Calcified coronary vessel

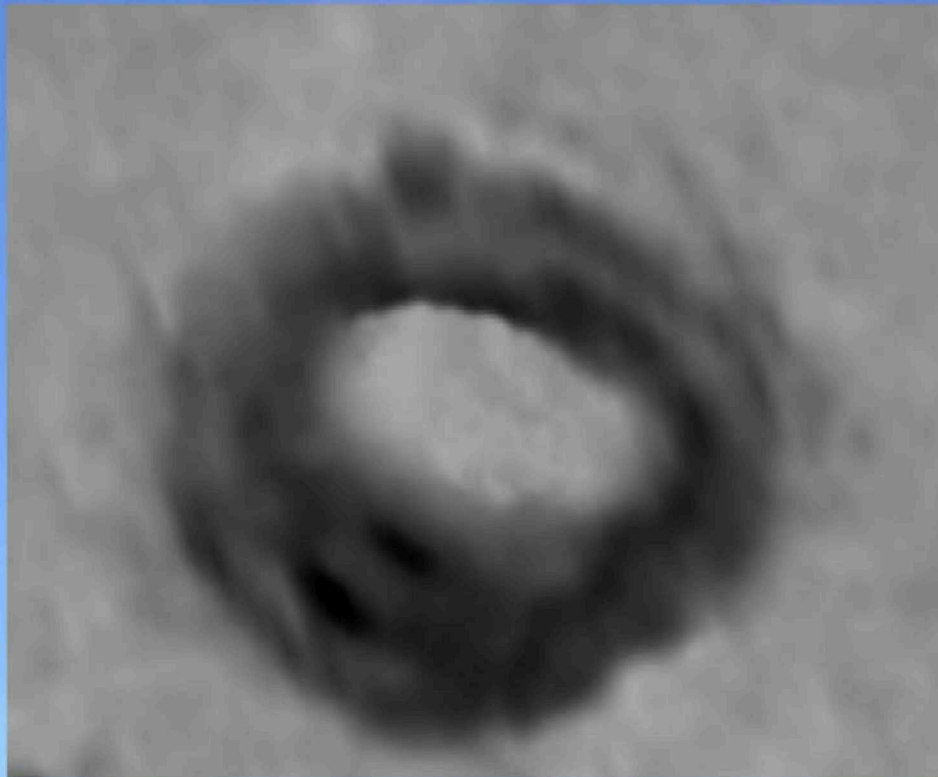


# 3D-Reconstruction of the calcification

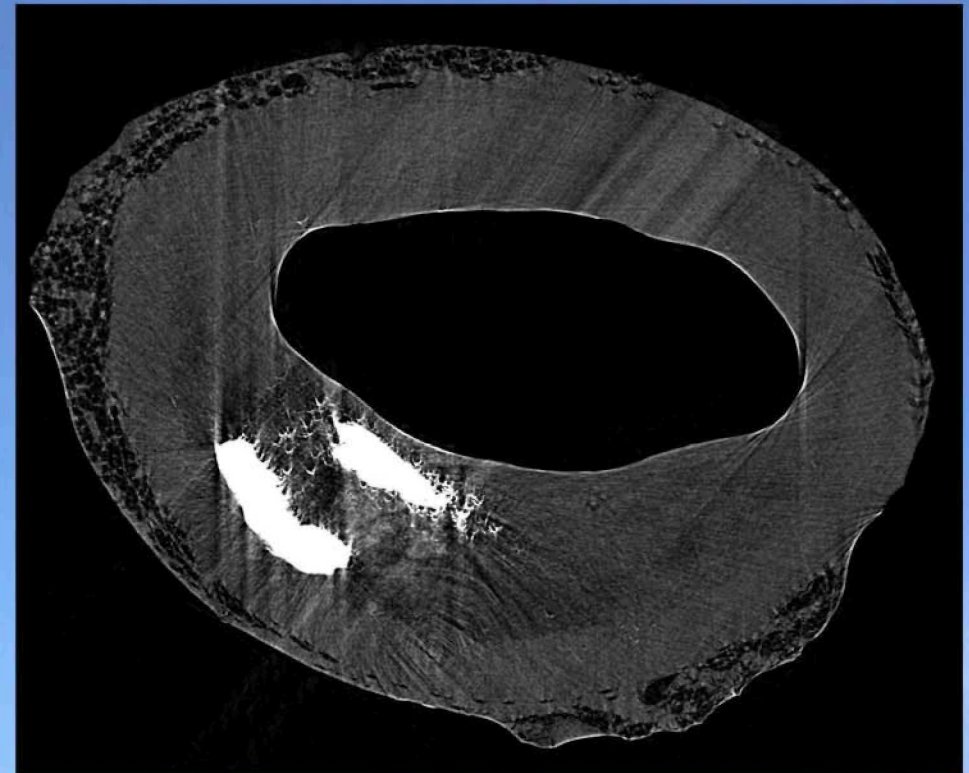


Courtesy of  
F.Schmid

# Comparison Between MR Imaging and $\mu$ -CT



MR image  
100x100x400 $\mu$ m



SR image (phase contrast)  
12x12x12 $\mu$ m

Courtesy of  
F.Schmid

# Acknowledgement

---

to the SYRMEP/SYRMA team:

A.Abrami, V.Chenda, D.Dreossi, L.Mancini, E.Quai, R.H. Menk,  
N.Sodini, F.Zanini  
*Sincrotrone Trieste*

F.Arfeffi, E.Castelli, R.Longo, L.Rigon  
*University and INFN Trieste*

P.Bregant, M.Cova, E.Quaia, D.Sanabor, M.Tonutti, F.Zanconati  
*Radiology Dept. and Health Physics – University and Cattinara  
Hospital Trieste*